Landslides DOI 10.1007/s10346-024-02316-7 Received: 16 January 2024 Accepted: 4 July 2024 © Springer-Verlag GmbH Germany, part of Springer Nature 2024

## Xiaojun Guo • Marcel Hürlimann • Peng Cui • Xiaoqing Chen • Yong Li

## Check for updates

# Monitoring cases of rainfall-induced debris flows in China

Abstract Debris flows are considered one of the most hazardous types of mass movement. China has a long history of monitoring debris flows, which has enhanced the understanding of debris flows and the development of strategies for their prevention. This study reviewed case studies and outputs related to debris flow monitoring in China. The monitoring systems are set in seven catchments, with area between 2 and 40 km<sup>2</sup>, covering various types of debris flows in different climate conditions. This review also introduced the definitions and classifications adopted for debris flows in China for comparison with those used in Western literatures. A comprehensive analysis was conducted of debris flow parameters, including the grain size distribution, density, Froude number, velocity-depth relationship, volume-peak discharge relationship, volume-drainage area relationship, and velocity and peak discharge calculation methods. Additionally, the rainfall intensity-duration thresholds were compared. Accurate identification of such information is fundamental for enhancing comprehension of debris flow characteristics, facilitating monitoring, and the implementation of early warning and alarm systems.

**Keywords** Debris flow · Monitoring · Definition and classification · Flow features · Empirical equations

#### Introduction

Debris flow is a phenomenon intermediate between landslides and fluvial sediment transport (Rickenmann 1999) and represents a major hazard in mountainous regions. They occur frequently in western China where there are topographic transitions, dense faults, strong tectonic activities, frequent earthquakes, deep-cut landforms, and fragile ecological environments (Cui et al. 2011, 2014). For example, debris flows in 2010 in Zhouqu (Gansu Province, Northwest China) resulted in 1765 fatalities (Cui et al. 2013), and debris flows in the Wenchuan earthquake area (Sichuan Province, Southwest China) have repeatedly destroyed structures and caused hundreds of human fatalities (Tang et al. 2012; Guo et al. 2016a; Yang et al. 2021).

In situ monitoring is fundamental for acquisition of the data for the dynamics of debris flows, early warning systems, and preventing structures. Numerous monitoring systems have provided valuable scientific data and facilitated comprehensive understanding of regional variations in debris flows over the world (e.g., Berti et al. 2000; Marchi et al. 2002; Hürlimann et al. 2003, 2014; Imaizumi et al. 2005; McArdell and Badoux 2007; Badoux et al. 2009; Suwa et al. 2009, 2011; Hübl and Kaitna 2010; Yin et al. 2011; Navratil et al. 2013; Comiti et al. 2014; Gregoretti et al. 2016; Palau et al. 2017; Coviello et al. 2019a, b). Typically, monitoring parameters are categorized into two groups: triggering factors and dynamic parameters. Precipitation, temperature, snow depth, channel water runoff, soil moisture,

pore pressure, and soil matric suction in potential source slopes fall under the category of triggering factors, and the dynamics parameters include flow depth, flow velocity, ground vibration, basal stress, and impact force (e.g., Arattano and Moia 1999, Arattano et al. 2015; Berti et al. 1999, 2000; Imaizumi et al. 2005; Itakura et al. 2005; Badoux et al. 2009; McCoy et al. 2010, 2012, 2013; Kean et al. 2011, 2013; Abancó et al. 2012, 2014, 2016; McArdell 2016; Cui et al. 2018). Measurements of relevant parameters can be obtained using either direct-contact or non-contact sensors (e.g., Hürlimann et al. 2019a, b). The non-contact approach is more secure but requires careful site selection to ensure effective collection of data. For example, ultrasonic, radar, laser devices and large-scale particle image velocimetry are widely used to measure flow parameters (e.g., stage and velocity) (Jacquemart et al. 2017; Hübl et al. 2009, 2018; Hübl and Mikoš, 2018; Cui et al. 2018; Marchetti et al. 2019; Coviello et al. 2019a, b; Wei and Liu 2020; Allstadt et al. 2020; Belli et al. 2022). Direct-contact monitoring devices are used to measure basal stress or impact force. They are often positioned in the middle of a channel, which makes them highly susceptible to damage (Wendeler et al. 2007; McArdell and Badoux 2007; Hübl et al. 2009; McCoy et al. 2010; Nagl and Hübl 2017; Nagl et al. 2018; Yan et al. 2023). Additionally, technological advancements have enhanced the appeal of certain monitoring devices. For example, geomatic and remote sensing techniques are increasingly utilized for detecting debris flow sources, while photography with unmanned aerial vehicles enables high-resolution topography reconstruction (e.g., Bremer and Sass 2012; Catani et al. 2014; de Haas et al. 2014; Cook 2017; Cucchiaro et al. 2018; Morino et al. 2019; Huang et al. 2021).

Benefiting from technological advancements, the scope of approaches applicable to monitoring debris flows is increasing steadily. Most devices can perform with satisfactory accuracy. However, obtaining effective data remains a challenge owing both to the sudden occurrence and destructive power of debris flows and to the harsh environmental conditions. In certain situations, manual approaches remain necessary. Particularly in the decades following the 1960s, manual observation played a crucial role in China. The flows monitored using manual approaches exhibited diverse behavior and a range of characteristics across different sites, even when compared with those of flow patterns globally.

This work provides a review of rainfall-induced debris flow monitoring in China, with an introduction of some special Chinese terminologies and classifications. Additionally, the characteristics, e.g., grain size distribution, density, and velocity of flows observed in monitoring basins, are analyzed, and the empirical formulas derived for calculation of velocity, discharge, and volume are introduced, together with the comparison of the rainfall thresholds. This work also compares the derived findings with those from other

Published online: 24 July 2024 Landslides

monitoring basins worldwide for a better understanding of debris flow characteristics specific to China.

#### **Definition and classification of debris flows in China**

Interpretation of debris flows in China has been subject to diverse perspectives and varying definitions. Generally, the descriptions provide an overview of two-phase (solid-liquid) flows that typically exhibit sudden onset, rapid movement, and relatively short duration; contain a mixture of water, fine clay particles, sands, and large boulders with a density of 1.2–2.3 g/cm³; and occur in gullies or on slopes. The liquid phase here represents a homogeneous slurry composed of water and fine sediment particles, whereas the solid phase consists of coarser particles (Chen et al. 1983; Qian and Wang 1984).

The behavior of a debris flow depends on the concentration of the solid component and the flow viscosity. A flow with low solid content and low viscosity exhibits turbulent characteristics similar to those of mountain flood. Conversely, a flow with high solid concentration and high viscosity may behave as a viscoplastic flow, generally intermittent and highly unstable in response to spatiotemporal variations of solid and water concentration (Chen et al. 1983). A debris flow has its own structure, specifically the initial shear strength that distinguishes it from a hyperconcentrated flow, and the fluidity, represented by the velocity gradient from the flow surface to the channel bed bottom, which serves as a crucial indicator for distinguishing it from a landslide (Wu et al. 1993).

The above definitions describe debris flows from the perspectives of occurrence conditions, formation and movement characteristics, fluid properties, and the features that differentiate them from other similar hazards (e.g., landslides and hyperconcentrated flows). The definitions are consistent with Western descriptions that define debris flows as "mixtures of debris and water with high sediment concentrations that move downslope as surging sediment slurries" (Coussot and Meunier 1996; Thouret et al. 2020) and "very rapid to extremely rapid flow of saturated non-plastic debris in a steep channel" (Hungr et al. 2001, 2014).

Flows that occur in steep mountain channels comprise water flows, hyperconcentrated flows, debris floods, and debris flows. In Western definitions, sediment concentration, grain size distribution (GSD), and/ or bulk density are the factors considered in distinguishing such flows (Vallance et al. 2000; Hungr and Jakob 2005; Vallance and Iverson et al. 2015). Water flows have a low sediment concentration generally < 4% by volume, which is insufficient to appreciably influence the rheological proprieties of the flowing water (Waananen et al. 1970; Brenna et al. 2020). Hyperconcentrated flows can be defined as turbulent to laminar and non-Newtonian fluids that have apparent liquid flow behavior (Pierson and Costa 1987; Costa 1988; Coussot and Meunier 1996), in which flowing water transports a substantial amount of suspended sediment, i.e., at least 20% but no more than 60% by volume (Beverage and Culbertson 1964). The boundary of the transition from water flow to a hyperconcentrated flow is defined as the onset of non-Newtonian fluid behavior, corresponding to a quantity of fines (< 0.063 mm) sufficient to maintain high viscosity and the intermittent suspension of large quantities of coarse material (Brenna et al. 2020). A debris flood is defined as a flow "during which the entire bed, possibly barring the very largest clasts, becomes mobile for at least a few minutes and over a length scale of at least 10 times the channel width" (Church and Jakob 2020). It is characterized more in the restricted sense of a

bedload-dominated phenomenon, whereas a hyperconcentrated flow is dominated by the suspended load (Manville and White 2003; Scheidl and Rickenmann 2010; Church and Jakob 2020). A debris flow is a sediment gravity slurry flow definable as the gravitational movement of a shearing, highly concentrated, yet relatively mobile mixture of debris and water. It comprises a sediment concentration that often exceeds 60% by volume, is a typical non-Newtonian flow with viscoplastic behavior, and has a plasticity index of < 5% in the sand and finer fractions (Pierson and Costa 1987; Costa 1984, 1988; Jakob and Hungr 2005). As a specific type, mud flow might contain a notable content of fines and exhibit measurably plastic behavior. The boundary is gradational and the plasticity index of the material is considered the controlling parameter (i.e., >5%; Hungr et al. 2001, 2014). The fluid properties of a stony debris flow, in which fine cohesive particles are absent or only available in a very small concentration, are close to those of water, and the flow dynamics are largely dominated by grain collision (Costa 1984; Gregoretti et al. 2019).

It is difficult to comprehensively compare the different terms of flow even in Chinese/Western literatures. This study conducted a first attempt of comparison and combination between the two points of view. The term "debris flood" is not commonly used in China. However, a similar classification of debris flow that is in common usage involves categorization based on rheological properties into three types of flow: dilute debris flow, subviscous debris flow ("quasi debris flow" in some literature, e.g., Tang et al. (2000), and Kang et al. (2004)), and viscous debris flow. To eliminate differences in recognition caused by classification methods and demarcations, a specific classification (Kang et al. 2004) is introduced as follows. Debris flows are classified into various types based on rheological properties, which primarily rely on two factors: flow density and clay-water ratio. Density represents the solid content within a flow, whereby a higher density indicates a greater concentration of solid particles and a denser structure with increased resistance to movement. The clay-water ratio refers to the proportion of clay (< 0.005 mm) in relation to the weight of the water, and it reflects the slurry properties of a debris flow; a higher ratio corresponds to the increased viscosity of the slurry. On the basis of those two factors, seven categories of flow can be distinguished: hyperconcentrated flow, diluted debris flow, subviscous debris flow, viscous debris flow, highly viscous debris flow, stony debris flow, and mud flow (Table 1 and Fig. 1).

A hyperconcentrated flow in China, which is defined as having a density of < 1.5 g/cm³ and fluid properties similar to those of clear water despite the higher sediment concertation, is different from the Western definition. A diluted debris flow, subviscous debris flow, viscous debris flow, and highly viscous debris flow all correspond to the Western classification of a debris flood and debris flow, but with more specific demarcation criteria. Because the defining limits of stony debris flows and mud flows are inherently arbitrary, they can be considered similar to those used in Western understanding. Except for hyperconcentrated flows, all other types fall within the research domain of debris flows used in China.

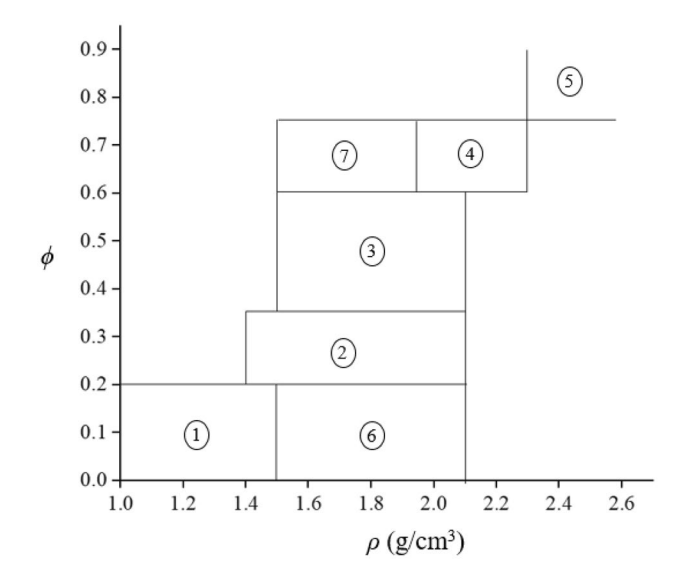
Notably, a debris flow is considered a type of landslide in the Western classification (Hungr et al. 2014). Mud flows, debris floods, and debris flows are different types, and each has a specific definition. In China, debris flows are considered a distinct geological hazard from landslides and are described as comprising a solid-liquid mixture, characterized by intermediate

Table 1 Chinese and Western classification of flow regime

Chinese classification				Western classification					
Term	д	<b>•</b>	Description	Term	Description	Φ,	Φ,,	д	Р
Hyperconcentrated flow	<1.5	< 0.2	Fluid properties are close to those of clear water despite higher sediment concentration	Hyperconcentrated flow	Suspension-dominated, turbulent to laminar and non- Newtonian fluids <sup>1,2</sup>	20–60%	40–70%³	1.3–1.8	< 5%
Diluted debris flow	1.5–1.7	0.2-0.5	Sands as suspended materials and boulders as bed load. t <sub>b</sub> , 2.0–7.0 Pa; η, 0.1–0.15 Pa·s	Debris flood	A bedload-dominated phe- nomenon, in the absence of high content of suspended sediment <sup>1</sup>	20–60%	40–70%³	1.3–1.8	< 5%
Subviscous debris flow	1.7–1.95	0.35-0.6	The fluidity has certain structural and viscous forces, is rippled, and is slightly turbulent.	Debris flow	A sediment gravity slurry flow definable as the gravitational movement of a shearing, highly concentrated, yet	%09<	70-90%³; 60-90%⁴	× 1.8	< 5%
Viscous debris flow	1.95–2.3	0.6-0.75	Boulders mixed well with the slurry, with low resistance. Velocity reaches 4–8 m/s. $\tau_{\rm br}$ 20–100 Pa; $\eta$ , 0.5–3.0 Pa·s		debris and water <sup>4</sup>				
Highly viscous debris flow	> 2.3	>0.7	Viscous and highly structural, huge resistance, very slow, creeping or laminar fluids						
Stony debris flow	> 1.5	<0.2	Grains > 2 mm account for more than 90%. Clay content is very small	Stony debris flow	Fine cohesive particles are absent. Fluid properties are close to those of water, and the flow dynamics are essentially controlled by grain collisions <sup>5</sup>	>20%			
Mud flow	> 1.5	>0.6	The opposite of a stony flow. Clay content is much higher than content of coarser particles	Mud flow	Solids are moved in suspension, and as bed load by fluid lift and drag, being measurably plastic <sup>5</sup>	>20%	40-70%³		> 5% <sup>5</sup>

Data source for Chinese classification is from Kang et al. (2004), while different sources are used for the western classification (Brenna et al. 2020<sup>1</sup>; Beverage and Culbertson 1964<sup>2</sup>; Costa 1984<sup>3</sup>; Johnson 1970<sup>4</sup>; Hungr et al. 2001, 2014<sup>5</sup>)

 $\rho$ , density,  $g/cm^3$ ;  $\phi$ , clay volume concentration, i.e., ratio of clay weight to water weight;  $\tau_b$ , yield stress, Pa;  $\phi$ , viscosity coefficient, Pa·s;  $\Phi_\nu$ , sediment content (by volume);  $\Phi_\nu$ , sediment content (by weight);  $P_\nu$ , plastic index



**Fig. 1** Chinese flow regime classification based on density  $\rho$  and clay volume concentration  $\phi$  ((1) hyperconcentrated flow, (2) diluted debris flow, (3) subviscous debris flow, (4) viscous debris flow, (5) highly viscous debris flow, (6) stony debris flow, and (7) mud flow). See descriptions in Table 1 for further details (Kang et al. 2004)

properties between common mountain floods and landslides. Additionally, the scope of a debris flow includes both stony debris flows with extremely low clay content and mud flows with exceptionally high clay content.

Irrespective of classification, debris flows generally encompass a continuum ranging from a hyperconcentrated flow to a debris flood and debris flow (or to dilute, subviscous, viscous, and highly viscous states). In practice, accurate demarcation of such flows in a small mountainous watershed remains ambiguous when using existing definitions, and it also poses a challenge in discerning specific parameter values. The most common phenomenon in a watershed is a flash flood that is occasionally accompanied by debris floods and sporadic debris flows with higher density and viscosity, depending on the triggering conditions (e.g., rainfall) and sediment availability. Even within one specific event, a sequence starting with a flash water flood, followed by either a debris flood or a debris flow, and ending with a water flood is generally observed.

There are other classifications of flow regimes from various perspectives used in China. For example, they can be classified as rainfall-induced, glacier and/or snowmelt-induced, and dam-break debris flows from the perspective of water sources (Kang et al. 2004), and as gravity-driven (also called landslide-triggered) and runoff-driven (also called channelized) flows from the perspective of the dominant triggering force (Yu et al. 2020). They can also be categorized as a continuous flow or a surge flow based on flow regime (Li et al. 2003, 2004).

## Rainfall-induced debris flow monitoring sites in China

Seven catchments around the Qinghai–Tibet Plateau highly prone to debris flows have been selected for monitoring sites. Three catchments are in the southwest and four in the northwest China (Fig. 2). Among them, Jiangjia Gully (JJG) is still actively observed, whereas the Ergou catchment was under monitoring during 2013–2019. The others, monitored during the 1960s and 1970s, are not currently monitored.

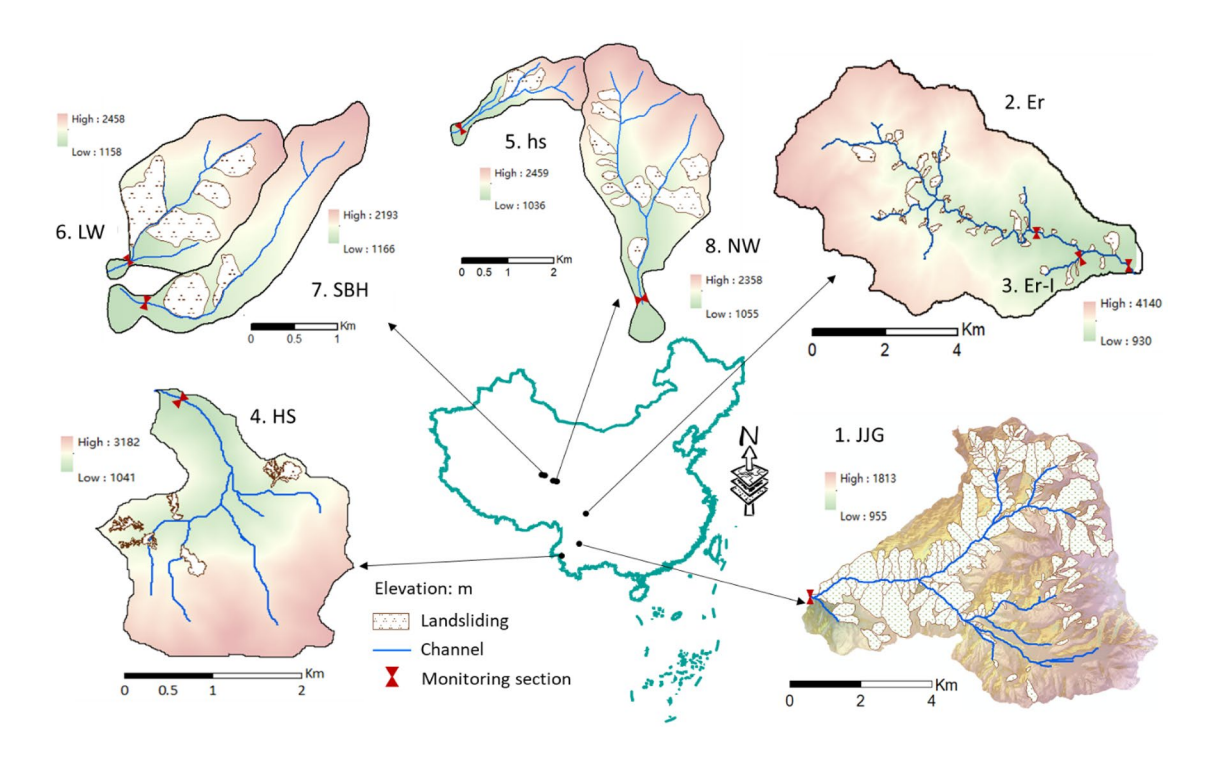


Fig. 2 Location, topography, and material source distribution of the monitoring sites in China

## 1. Jiangjia Gully in the Xiaojiang River

The JJG is representative of the characteristic occurrence of debris flows in the dry hot Xiaojiang River valley in Southwest China. Owing to its frequent debris flow activity (typically 10–20 events annually, with a maximum of 28 events in 1 year), the catchment is often referred to as a "debris flow museum."

The catchment size is approximately 48.6 km², and the channel length is approximately 15 km. The highest and lowest elevations are 3269 and 1042 m, respectively. The area has a semiarid climate, with mean annual precipitation (MAP) of 400−600 mm at the outlet and ≈1000 mm in the headwater region. Because of intense regional tectonic activity, the exposed rocks within the watershed exhibit high degrees of fracturing and metamorphism. The rocks are characterized by weakness, notable weathering, fragmentation, and widespread distribution of colluvium and mantle rock throughout the slopes and channels. The accumulation of clastic detritus serves as the primary source material for debris flows.

The monitoring section is situated within the catchment, while the controlling area spans approximately 33.4 km². Since its establishment in the 1960s, the monitoring system has undergone extensive testing, and it remains operational to this day, having amassed a vast database that encompasses over 600 debris flow events. The monitored debris flows exhibit viscous behavior and have high density (up to 2.4 g/cm³), accompanied by noticeable surges during each event (Li et al. 2003, 2004; Guo et al. 2020).

Since the 1990s, ten rain gauges have been installed throughout the watershed to provide rainfall observations. The data collected by these gauges at the source headwater are automatically transmitted in real time via the General Packet Radio Service. The dynamic parameters of the debris flows are the primary observation output, and most parameters are observed using semiautomated approaches. The objective measurements include debris flow occurrence time, duration, depth, and velocity. Traditionally, flow velocity was measured by timing the passage of the flow through a 200-m straight channel. For most surges, depth was manually determined using cross-sectional markers. Samples taken from the flow body were analyzed for density and rheology.

## 2. Ergou catchment in the Wenchuan earthquake area

The Ergou catchment (Er) is situated approximately 6 km NNE of the epicenter of the 2008 Ms 8.0 Wenchuan earthquake. The catchment encompasses an area of 39.4 km<sup>2</sup> and features a channel length of approximately 11.5 km. The headwater elevation stands at 4120 m, gradually decreasing to 990 m at the watershed outlet.

The topography exhibits typical characteristics resulting from tectonic uplift and subsequent fluvial erosion, with granite and sandstones being the predominant exposed rock types. Coseismic and subsequent landslides and collapses have produced loose colluvium in the channel and lateral slope deposits as the primary sources of material for debris flows.

The annual average precipitation near the catchment outlet is 1200 mm (Guo et al. 2016b; Cui et al. 2018). The monitoring system in the Ergou catchment was established during 2013–2019 (Cui et al. 2018). Four rain gauges were installed along the main channel and tributaries. Three hydrological stations were established on

the tributaries (the upstream area of the Ergou catchment, with an area of 32.4 km², and on a tributary Er-I, with an area of 2.34 km²) and at the outlet to monitor the hydrographs. Surface flow velocity and flow depth were monitored using radar speed indicators and ultrasonic stage meters, and the data were transmitted in timely via the General Packet Radio Service and the BeiDou Navigation Satellite System.

#### 3. Hunshui Gully in the Dayangjiang River

The Hunshui Gully (HSG) was monitored to investigate the characteristics of high density mud flows in the Daying River valley in southwestern Yunnan Province (Zhang and Liu 1989). Over 50 debris flows were recorded between 1974 and 1976. The catchment is a funnel-shaped basin with an area of 4.5 km² and a channel length of approximately 3.75 km. The highest and lowest elevations are 1820 and 958 m, respectively.

The region has a humid climate with a MAP of 1500 mm. The headwater tributaries account for 36.5% of the entire catchment area, with an aggregate landslide extent of 1.65 km². Most major tributaries follow NE–SW trending faults that coincide with the locations of these landslides. Investigation revealed that the uppermost layer, about 3–4 m in depth, of the slopes consists of weathered soils with high clay content, and the underlying layer is a sliding layer composed of clayed schist, extending to a depth of approximately 35 m. Landslides and surface runoff erosion were the primary sources of debris flow.

The flow parameters were manually measured, i.e., flow velocity was determined using a stopwatch, and depth was referenced to a cross section. Density and rheological parameters were analyzed from samples taken from the moving flow body.

## 4. Four monitoring sites along the Bailong River

The Bailong River (BL) is on the northeastern edge of Qinghai–Tibet Plateau. It is an earthquake-prone region with an arid climate (MAP, 360–660 mm). The river is deeply incised, with steep slopes mantled by friable and weak rock outcrops owing to frequent seismic activity. The watershed is of low vegetation coverage vegetation and the channels contain abundant Quaternary alluvial deposits, especially debris flow deposits, as well as weathered residues and slope deposits.

In the 1960s, debris flow was monitored in four BL catchments: the Niwan (NW), Liuwan (LW), Shanbeihou (SBH), and Huoshao (hs) catchments. Manual methods dominated the measurement of flow parameters. The debris flows exhibited high viscosity, high density, and frequent surges.

The geographic parameters of the monitored catchments are listed in Table 2.

#### 5. Comparison of the catchments

Usually, morphometric parameters such as basin area and watershed/fan slope are used for distinguishing the dominant flow type of a drainage basin. Catchments are typically categorized into different classes based on the dominant flow process (i.e., fluvial,

Table 2 Main parameters of the monitored catchments (taking the monitored section as the outlet)

5. hs	Name (abbreviation)	Area (km²)	MAP (mm)	Mean channel gradient (%)	Channel length (km)	Basin elevation difference (m)	Monitoring period
1	Jiangjia (JJG)	33-4	400-1000	11.5	12.0	2227	1961-
2	Ergou (Er)	39.4	1000-1200	14.6	11.5	3130	2013–2019
3	Ergou-l (Er-l)	2.4	1000-1200	28.0	2.6	1900	2013–2019
4	Hunshui (HSG)	4.5	1500-1800	13.6	3.8	862	1975–1976
5	Huoshao (hs)	1.98	400-600	48.0	1.4	1303	1969–1975
6	Liuwan (LW)	1.97	400-600	29.0	1.2	1028	1963–1964
7	Shanbeihou (SBH)	2.18	400-600	31.0	1.7	1300	1966–1967
8	Niwan (NW)	10.3	400-600	23.0	5.3	1423	1965–1967

mixed, or debris flow) by analyzing the relationship between the Melton Index and other topographic parameters such as fan slope (Bardou 2002; Wilford et al. 2004; Bertrand et al. 2013). The Melton Index, calculated as the ratio of catchment relief to the square root of the catchment area, reflects the gravitational potential, whereas the fan slope indicates the dominant transport process resulting from past flows (Bertrand et al. 2013). This classification provides a crucial reference of debris flow susceptibility.

We compared the Melton Index with the fan slope of the seven monitored sites and that of other sites worldwide, i.e., Chalk Cliffs (CC), Gadria (Ga), Moscardo (Mos), Illgraben (Il), Kamikamihorizawa (Ka), Lattenbach (La), Réal (Réa), Rebaixader (Reb), and Shenmu (Sh) (Coe et al. 2008; McCoy et al. 2010, 2013; Kean et al. 2013; Marchi et al. 2002; Comiti et al. 2014; Coviello et al. 2019a, b; Badoux et al. 2009; McArdell and Badoux 2007; McArdell 2016; Suwa et al. 2009, 2011; Hübl and Kaitna 2010, 2018; Okano et al. 2012; Navratil et al. 2013; Hürlimann et al. 2014, 2019a, b; Abancó et al. 2012, 2016; Bel et al. 2017; Huang et al. 2013, 2017). The classification of most catchments is reasonable, in that all the catchments in China and most of the other catchments are unsurprisingly categorized as having a mixed and/or debris flow regime. Among the seven Chinese catchments, the Er-I catchment has a smaller area but higher Melton Index and is classified into only debris flow regime, similar to the Reb catchment.

The calculation of the Melton Index relies strongly on drainage area (i.e., the larger the basin, the smaller the Melton Index), and it is exemplified when comparing the Ergou catchment with the Er-I tributary, which is similar in terms of catchment relief but with notably different size (i.e., 39.4 km² versus 2.4 km²). Consequently, according to the classification, the Ergou catchment exhibits characteristics similar to those of a fluvial regime, whereas the Er-I tributary is more closely associated with a debris flow regime. This finding, which aligns with our current understanding and reflects reality, is also evidenced by the performance at the Sh site and its tributary (Sh-A), with catchment sizes of 72.1 and 4.0 km², respectively (Huang et al. 2013).

The formation process of a debris flow is influenced not only by topographic conditions but also by sediment availability. For example, the classification methods also cause some incorrect cases with large sizes and abundant loose materials, e.g., the JJG and NW

catchments, which are typical debris flow catchments, classified as mixed and close to the fluvial regime in Fig. 3. This underscores the challenges and uncertainties in distinguishing debris flows. The classification methods based on morphological features are derived from typical cases and serve only as reference for assessment purposes, and special consideration should be given to those with unique local characteristics.

## Monitoring output and debris flow features

#### Grain size distribution and bulk density

Rheological behavior of a flow can also be distinguished by the GSD, especially the fine fraction, which is indicative of the mechanical properties of a debris flow. It is an important parameter that can help practitioners choose an appropriate rheological law when conducting site-specific hazard zoning (Bardou et al. 2003; Hürlimann et al. 2019a, b). Based on the clay and matrix contents, flows can be categorized into two primary rheophysical classes: the viscoplastic class, characterized by Herschel–Bulkley or Bingham flow behavior, and the collisional frictional class that exhibits Coulomb-like flow behavior (Bardou et al. 2003). The former class is referred to as muddy debris flows, whereas the latter class is known as stony debris flows.

Here, GSD curves were derived from samples collected from the matrix of debris flow deposits in the Ergou catchment and from the moving bodies of debris flows at other sites. We plotted GSD curves with a maximum grain size of 20 mm (Fig. 4), to facilitate the assessment of distinct curves and allow comparison with the classification of Bardou et al. (2003) and the results of Hürlimann et al. (2019a, b).

Most of the monitoring sites are characterized by a mixed and/ or debris flow regime, except for Shenmu and Ergou (the two largest catchments), which are defined as fluvial catchments (Fig. 4). The particle composition in the Ergou catchment differs markedly, with less clay and more coarse gravels, making it better suited to a collisional–frictional regime, where the flows behave more like stony debris flows or debris floods, as confirmed by video footage obtained in the Ergou catchment (Cui et al. 2018). The debris flows in Ga-1 and CC fall in the range of those in the Ergou catchment.

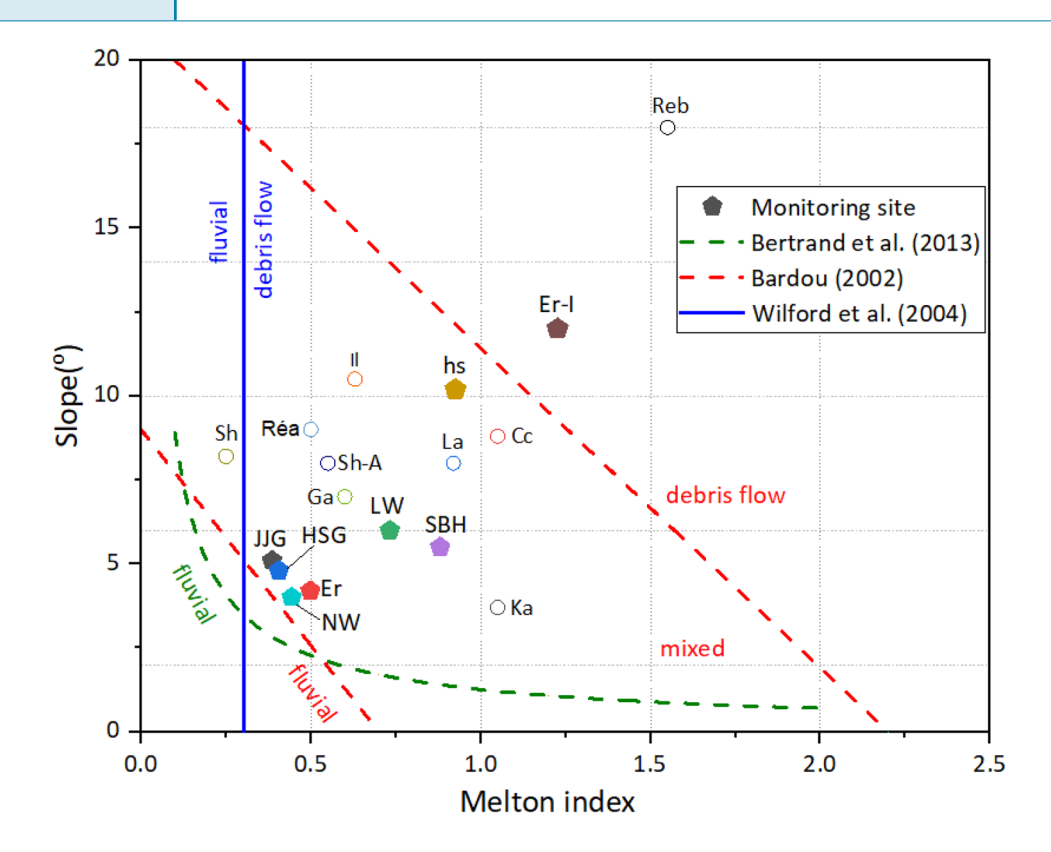


**Fig. 3** Relationship between the Melton Index and fan slope of the seven Chinese monitoring sites and other monitoring sites worldwide (adapted from Hürlimann et al. 2019a, b): CC, Chalk Cliffs; Ga, Gadria; Mos, Moscardo; II, Illgraben; Ka, Kamikamihorizawa; La, Lattenbach; Réa, Réal; Reb, Rebaixader; and Sh, Shenmu. See Table 2 for abbreviations of Chinese sites

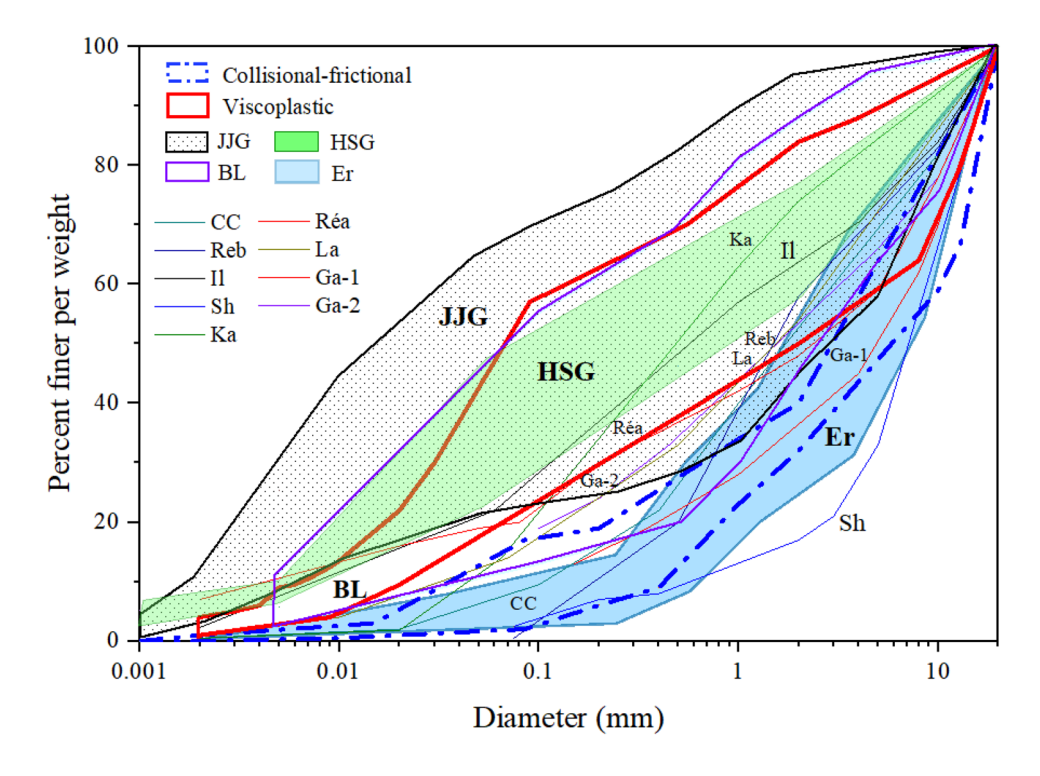


**Fig. 4** Grain size distributions of flows sampled at monitoring sites. Samples from JJG, HSG, and BL catchments were collected from the body of the moving flow; samples from the Ergou catchment were taken from deposits

Compared with the grain composition at other sites, the GSDs in JJG exhibit a notably broader spectrum (ranging from clay to gravel), despite differences in test materials (debris flow moving body versus deposit). Many GSDs in JJG exceed the upper limit of the viscoplastic flow range, suggesting that debris flows contain a higher proportion of clay and fine sands. The lower parts of the GSDs also fall into the range of the collisional–frictional regime, indicating a higher level of diversity in debris flow compositions.

The grains in HSG, which are concentrated within a specific range, are predominantly composed of clay and fine sands. The four BL tributaries exhibit characteristics that are transitional between those of JJG and HSG, whereas the characteristics of most other sites compared are within those of the BL and HSG regions, indicating similar regimes characterized by viscoplastic flows. The ranges also coincide with debris flows in most of the other international sites, as shown in Fig. 4. It should be noted that the data from the international sites reflect specific cases from the literature and are not as comprehensive as those from Chinese sites.

Bulk density ( $\rho$ ) is the sum of fluid density ( $\rho_f$ ) and solid component density ( $\rho_s$ ), ranging from 1.3 to 2.4 g/cm³ for hyperconcentrated flows and debris flows (Pierson 1980; Zanchetta et al. 2004). The maximum density of the JJG and BL flows was measured at 2.4 g/cm³, indicating a high proportion of solid components. The flow density recorded in HSG typically falls within the range 1.90–2.24 g/cm³. However, in the Ergou catchment, although the maximum flow density was recorded by field investigation at 2.16 g/cm³ on July 10, 2013 (Guo et al. 2016a), it has not exceeded 1.85 g/cm³ since 2014 within the monitoring period, with most cases in the range of 1.3–1.8 g/cm³, showing a lower solid component and indicating temporal variation of post-earthquake debris flows (Guo et al. 2021b).

#### Flow velocity

## 1. Flow velocity-depth relation

The velocity (u, m/s) of a flow can be decomposed into two components: surface velocity  $u_{surf}$ , the instantaneous velocity of the flow surface, and travel velocity  $u_r$ , corresponding to the total velocity of the flow body. Among the monitoring sites, debris flows in two sections were measured manually using a stopwatch to determine  $u_r$  at JJG, HSG, and the four BL monitoring sites, whereas  $u_{\text{surf}}$  was measured using radar speed indicators in the Ergou catchment. Velocity decreases vertically; therefore,  $u_{\text{surf}}$  is generally larger than  $u_r$ . It is suggested that a linear relation exists between the two components, i.e.,  $u_r = k u_{surf}$ , where k is a constant (<1) (Hungr et al. 1984; Takahashi 1991). This was verified by comparison of the values for the two components measured in JJG, which revealed a strong linear relationship, i.e.,  $u_r$  measured using the stopwatch generally yielded smaller values than  $u_{\text{surf}}$ obtained from radar testing (with k falling within the range of 0.4-0.8; average, 0.53), as shown in Fig. 5.

Flow velocity is influenced by many factors, e.g., flow type, flow height, channel slope, and roughness. Different catchments clearly exhibit varying velocities within their flows. In the Ergou and HSG catchments, the typical flow velocity remains below 6 m/s; however, in the BL catchments, owing to the steeper channel gradient, the flow can reach higher velocities of 8–9 m/s (Fig. 6). Moreover, in JJG events, it is not uncommon for flow velocities exceeding 10 m/s, despite the gentler channel slope. On one hand, these findings reflect the homogeneity of a flow with lower internal resistance. On the other hand, it is proposed

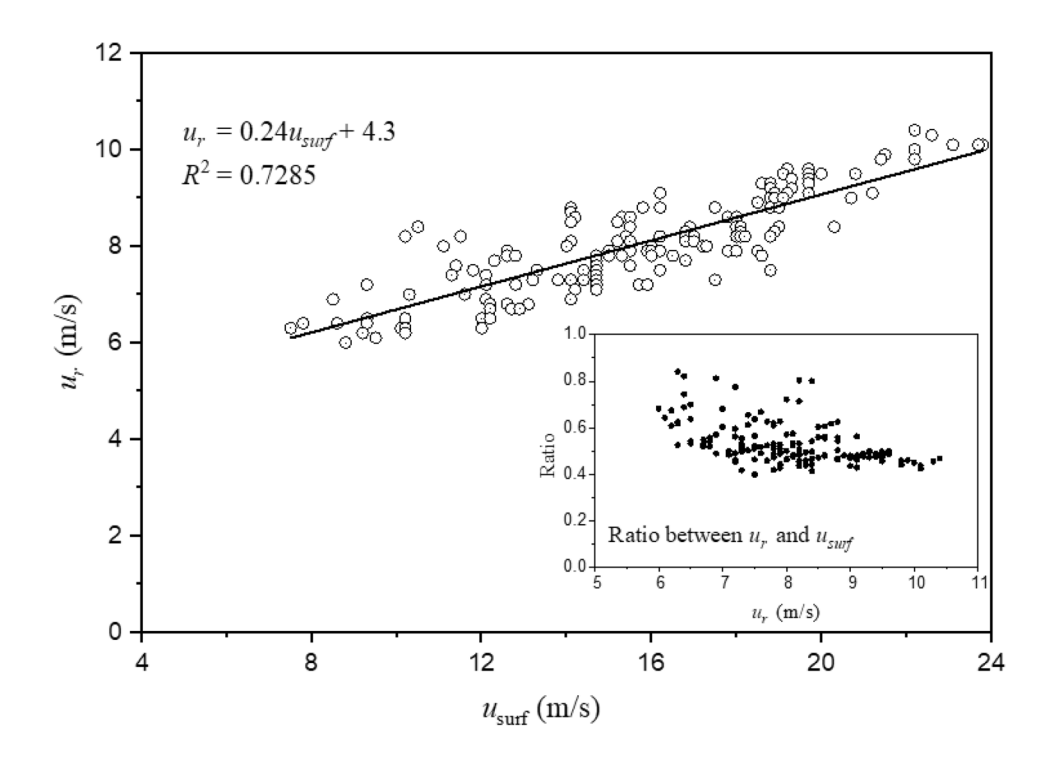


**Fig. 5** Relationship between monitored travel velocity  $(u_r)$  and surface velocity  $(u_{surf})$  in JJG

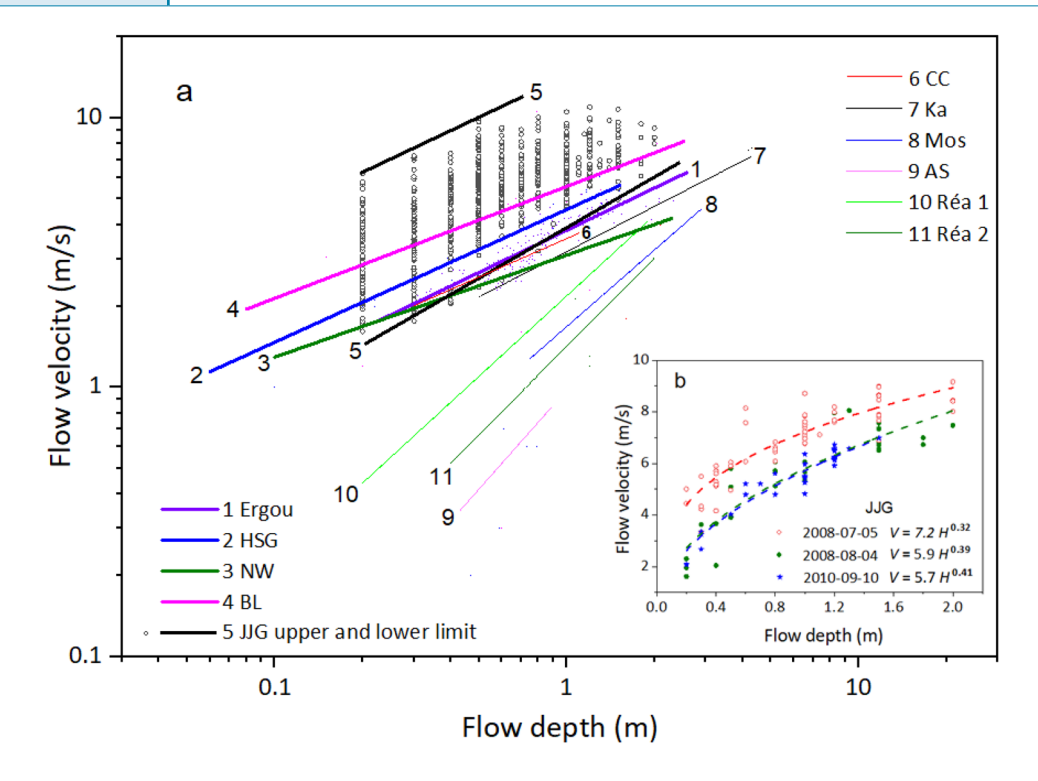


Fig. 6 Flow velocity and flow depth relationships for **a** the Chinese and other catchments and **b** three events in JJG (data sourced from Marchi et al. (2002), Kean et al. (2011), McCoy et al. (2011), Navratil et al. (2013), and Okano et al. (2012)). See Fig. 3 and Table 2 for abbreviations of sites

that the initial surge of a debris flow reshapes and smooths the channel bed, i.e., the co-called "paving way process," which contributes approximately 30% of the reduction in resistance during movement and ultimately leads to notably higher flow velocity (Wang et al. 2001; Hu et al. 2004; Chen et al. 2023).

Empirical relationships between flow velocity and flow height are crucial in identifying flow discharge through field investigation. These relationships are expressed as power functions across all catchments (Table 3 and Fig. 6a). The relationship in HSG exhibits a particularly statistically significant correlation that is possibly attributed to the concentrated grain composition of the muddy fluids. In the Ergou catchment, the correlation of the relationship is also statistically significant but it exhibits a slower rate of increase. Furthermore, there is a distinct inflection point at 1 m, which can be attributed to the transition in flow type. When the water depth is <1 m, the predominant flow is characterized by water movement; however, when the flow depth exceeds 1 m, it transforms into a hyperconcentrated flow or debris flood with an increased presence of solid particles. Consequently, this leads to an increase in internal flow resistance.

Despite analysis of the 640 surges in JJG, a general relationship was very difficult to derive; however, distinct upper and lower limits for the relationship were determined (Fig. 6a). Meanwhile, evident power relationships could be identified for individual events, even with different exponents and coefficients, as depicted in Fig. 6b. This is comprehensible because of the potential variations in flow types.

The four BL catchments were categorized into two groups: NW, typified by larger size and much lower channel slope, and the other three catchments grouped together based on their smaller size and higher channel slope. The corresponding results, listed in Table 3 and illustrated in Fig. 6a, show that the relationship for the latter group is much higher than that for NW.

The relationships for the Ergou catchment and NW are consistent with those for Ka and CC and higher than those for Mos, AS, and Réa (Fig. 6). This result might include uncertainties attributable to differences in channel conditions (such as slope) and data sources, i.e., we use real-time monitoring data, whereas analyses for other sites rely on representative values of events or surges. For example, the peak flow stage and average flow  $u_r$  through the basin are used in AS (Kean et al. 2011),  $u_r$  (estimated using a geophone) and peak height are used in Mos and Réa (Marchi et al. 2002; Navratil et al. 2013), and peak  $u_{surf}$  and peak height are used in Ka (Okano et al. 2012).

The relationship between velocity (u) and depth (H) is also reflected by the dimensionless Froude ( $F_r$ ) number, which describes the stability of a deformable flow surface as the ratio between inertial and gravitational forces acting on the flow (Manville et al. 1998). In subcritical flows ( $F_r < 1$ ), runoff will be deep and slow with a flat and smooth surface, whereas in supercritical flows ( $F_r > 1$ ), runoff will be shallow and fast, exhibiting waves and disturbances such as hydraulic jumps (Manville et al. 1998). The relationships between  $F_r$  and the flow height in the monitored catchments are shown in Fig. 7.

**Table 3** Flow velocity and flow depth relationship for Chinese and other monitoring sites

Catchment	Relation	R²	Source	Line no
Ergou	$u_{\rm surf} = 3.82 H^{0.52}$	0.8298		1
HSG	$u_{\rm r} = 4.56 H^{\rm o.49}$	0.8908	Zhang and Liu (1989)	2
NW	$u_{\rm r} = 3.09 H^{0.38}$	0.6124	Li and Zeng (1982)	3
Other three sites in BL	$u_{\rm r} = 5.56 H^{0.42}$	0.4301	Li and Zeng (1982)	4
JJG-upper limit	$u_{\rm r} = 10.63 H^{0.31}$	0.9248		5
JJG-lower limit	$u_{\rm r} = 3.70 H^{0.80}$	0.9056		5
CC	$u_{\rm r} = 3.60 H^{0.50}$			6
Ka	$u_{\rm surf} = 0.28 H^{1.34}$	0.8203	Okano et al. (2012)	7
Mos	$u_{\rm r} = 1.68 H^{0.95}$	0.8363	Marchi et al. (2002)	8
AS	$u_{\rm r} = 0.97 H^{1.22}$	0.3741	Kean et al. (2011)	9
Réa-1	$u_{\rm r} = 2.18 H^{0.99}$	0.5972	Navratil et al. (2013)	10
Réa-2	$u_{\rm r} = 1.42 H^{1.09}$	0.6173	Navratil et al. (2013)	11

The horizontal lines in Fig. 7a represent the average  $F_{\rm r}$  of a catchment based on the acquired data. The  $F_{\rm r}$  values in the Ergou catchment and HSG exhibit comparably low levels of variability, with standard deviations of 0.14 and 0.20, respectively, indicating a higher degree of flow homogeneity. These values fall within the

ranges of 0.96–1.63 (average, 1.24) and 1.01–2.01 (average, 1.47), respectively, consistent with the fact that these flows are shallow, fast-moving, water-dominated systems subject to disturbances. The values are close to those for Ka and Ga (Okano et al. 2012; Comiti et al. 2014; Coviello et al. 2019b) and higher than those in Mos and

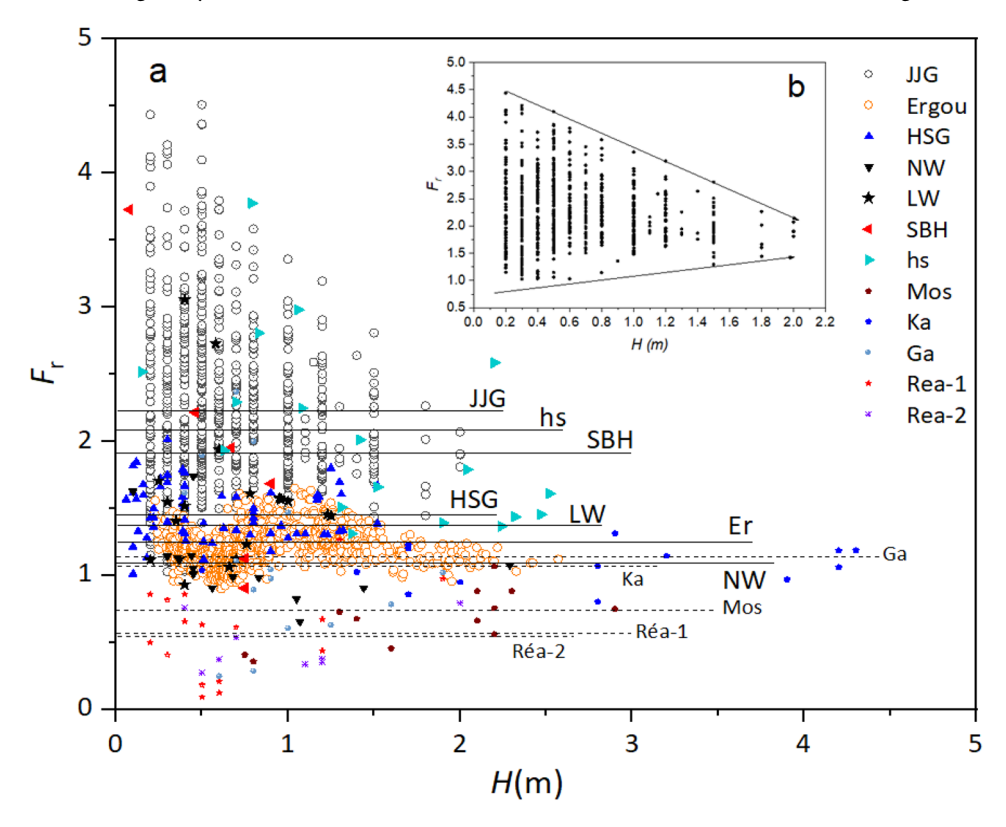


**Fig. 7** Froude number  $(F_r)$  versus flow depth (H) of debris flows in Chinese monitored catchments: **a** the distribution of  $F_r$  values based on data collected from the catchments, where the horizontal lines represent average values, and **b** the distribution of  $F_r$  values in JJG

Réa (Marchi et al. 2002; Navratil et al. 2013). This is attributable to the flow regime in which a viscous debris flow generally has a much higher  $F_{\rm r}$  value than that of either a mud flow or a debris flood. Additionally, the different data sources of velocity and flow height also result in the variation.

Compared with the  $F_{\rm r}$  values of the other three BL catchments, the  $F_{\rm r}$  value of NW is smaller, i.e., in the range of 0.65–1.73, with a standard deviation and average value of 0.27 and 1.09, respectively. In contrast, the values in the other three catchments (i.e., LW, SBH, and hs) are higher at 1.37, 1.93, and 2.07, respectively, with notably larger standard deviations. We hypothesize that a greater standard deviation indicates higher diversity in debris flows within the catchments; thus, these values reflect increased disturbance and diversity.

The debris flows in JJG exhibit distinctiveness characterized by a wide range of  $F_r$  values with a standard deviation of 0.63, which is notably higher in comparison to that of the other monitored catchments. Consequently, the average value holds little importance, although it is higher than the others. In Fig. 7b, increasing centrality is evident in the  $F_r$  value with increasing flow depth. This phenomenon might be attributable to similarities in the hydrodynamic characteristics during large-scale debris flow events (with high flow height), whereas smaller events display greater diversity. Despite the uncertainty, both the u-H relationship and the  $F_r$  value are higher in viscous debris flows (JJG and BL) and lower in mud flows and collisional–frictional flows (e.g., the Ergou catchment).

## 2. Empirical equations for flow velocity calculation

Flow velocity is influenced not only by flow height but also by channel slope and flow resistance. Most equations proposed for mean velocity and flow resistance are based on empirical data from prototype flows or measured velocity profiles in laboratory experiments. The following analysis primarily uses real monitoring data of the mean translational velocity between two sections in the field.

With the hypothesis that flow velocity could serve as a governing parameter for water-driven flows in steep environments, the mean velocity of a debris flow is commonly approximated using similar formulas to those employed for water flows (Rickenmann

1991). The commonly used formulas for Newtonian turbulent flows are typically expressed in the general form of  $V = CH^{\alpha}S^{\beta}$ , where V (m/s) is the flow velocity, H (m) is the flow depth, S is the channel gradient, and  $\alpha$  and  $\beta$  are coefficients. Additionally, the Manning–Strickler equation and the Chezy equation are the most popular forms of specific expression:

$$V = (1/n)H^{2/3}S^{1/2}$$
 Manning – Strickler equation (1)

$$V = CH^{1/2}S^{1/2} \quad Cheezy \ equation \tag{2}$$

where n is the roughness coefficient and C is the Chezy coefficient. The formulas derived for calculating the mean velocity of debris flows in China, based on the equations and monitoring data, are listed in Table 4.

Generally, negative correlation exists between the roughness coefficient (n) and the flow depth (H), and the value of n varies across different regions because it reflects flow resistance, which can be divided into external and internal components, with the former influenced by channel conditions and the latter mainly determined by flow composition. As per the standard equations, it is n that governs the calculation of velocity. Apart from curvature and blockage effects, the flow regime also has a notable impact on roughness, which can be classified into the following three categories.

- Low resistance: It is exemplified by the debris flows in JJG. The solid materials primarily originate from sufficiently weathered soils on the slopes, which are thoroughly mixed within the water to produce a relatively homogeneous composition of flow with small internal resistance. Moreover, the viscous debris flow has the ability to pave the way and reduce the external resistance of the channel, ultimately leading to notably higher flow velocity (Wang et al. 2001; Chen et al. 2023).
- Intermediate resistance: This is exemplified by the debris flows in the BL catchments, which also exhibit characteristic viscosity. The solid materials primarily originate from weathered substances on slopes. However, there is less weathering and a

Table 4	Equations	proposed for	estimation of the	mean velocity	of debris flows in China
---------	-----------	--------------	-------------------	---------------	--------------------------

	Formula	Note	Source
JJG	$V = (1/n)H^{2/3}S^{1/2}$	$1/n = 28.5  H^{-0.34}$	Kang (1985)
	$V = (m_c/a)H^{2/3}S^{1/2}$	$m_{\rm c}$ =75 $H^{-0.425}$ ; $a$ =( $\phi\gamma_{\rm H}$ +1), $\phi$ =( $\gamma_{\rm c}$ -1)/( $\gamma_{\rm H}$ -1) $m_{\rm c}$ and $a$ represent the external and internal components of the resistance, respectively; $\gamma_{\rm c}$ and $\gamma_{\rm H}$ are the densities of debris flow and solid materials, respectively (g/cm <sup>3</sup> )	Kang (1985)
BL	$V = 65KH^{1/4}S^{4/5}$	K is a coefficient ≈ 0.7	Yang (1985)
	$V = (1/n) H^{1/3} S^{2/3}$	$\it n$ is recommended in the range of 0.035–0.22 in the monitored catchments	Li and Zeng (1982)
	$V = (m_c/a) H^{2/3} S^{3/8}$	$m_{\rm c}$ = 15.5, for diluted debris flows	Li and Zeng (1982)
Ergou	$V = (1/n)H^{2/3}S^{1/2}$	$n \in [0.064, 0.121]$ , best fitted as 0.08	Cui et al. (2018)
HS	$V = (1/n)H^{2/3}S^{1/2}$	$n \in [0.032, 0.056]$ , with mean value of 0.041	Zhang and Liu (1989)
	$V = (1/n)H^{0.48}S^{1/2}$	n is recommended as 0.476	Zhang and Liu (1989)

- wider range of particle sizes, resulting in less-uniform mixing in comparison with that of the flows in JJG. Although a certain level of paving the way exists, it is not a prominently evident process in most cases.
- 3. High resistance: The continuous flows in the Ergou catchment and HSG exhibit relatively high resistance. The materials, originating from landslides and collapses, have accumulated in the channels over time. The two-phase flows are primarily influenced by surface water runoff, causing the transportations and collisions of large rocks and soil particles, and resulting in a notable level of internal resistance. Moreover, the rough channel bed also imposes a high level of external resistance.

#### Debris flow volume-drainage basin relationship

The total volume of debris flow (*M*) is crucial for evaluating potential hazards and designing mitigation structures. Generally, the volume is related to the basin area and varies with probabilities/recurrence intervals. We categorized the catchments into groups by their size and compared the values to those of similar-sized catchments worldwide (Fig. 8).

In China, debris flows are monitored only in catchments larger than 1 km². Among the four objective catchments with a size of approximately 2 km² (i.e., LW, hs, SBH, and Er-I), all volumes exceed the 50th percentile line proposed by Marchi (2019a). In catchments with an area in the range 3–10 km², the average value

of HSG is similar to that of La and higher than that of Ga, with a wider range and larger volumes. The relationship for NW is comparable to that for Il, and it also exhibits a wider range. For catchments with an area  $> 30~\rm km^2$ , such as Ergou and JJG, the mean volume is greater than that for Sh. The debris flow relationship in JJG has a notably broader range and the highest maximum value.

The maximum and average volumes of all Chinese sites, as well as the minimum volumes of the largest basins, fall within the range defined by D'Agostino and Marchi (2001). However, for a given catchment size, most data exhibit a higher debris flow volume in comparison to that of most other sites, resulting in a fitting line higher than the 50th percentile line proposed by Marchi (2019a). The best fitting line is also higher than the 50th percentile line of the PWRI (1988), which is used in Japan and Taiwan, for the condition of catchment size of > 4.5 km², especially for big catchments (size, > 30 km²). From another perspective, the maximum volumes are all much higher than those of the comparison sites, as recorded, indicating that the potential risk is much higher. Some of the maximum values exceed the 95th percentile line of the PWRI (1988) but remain within the envelopes of both D'Agostino and Marchi (2001) and Marchi et al. (2019a).

The Ergou and Er-I catchments exhibit evidently higher volumes, which can be attributed to the debris flood regime, where only very large events behave as debris floods/flows and reach the monitoring stations. This also explains the relatively narrow range (Fig. 8).

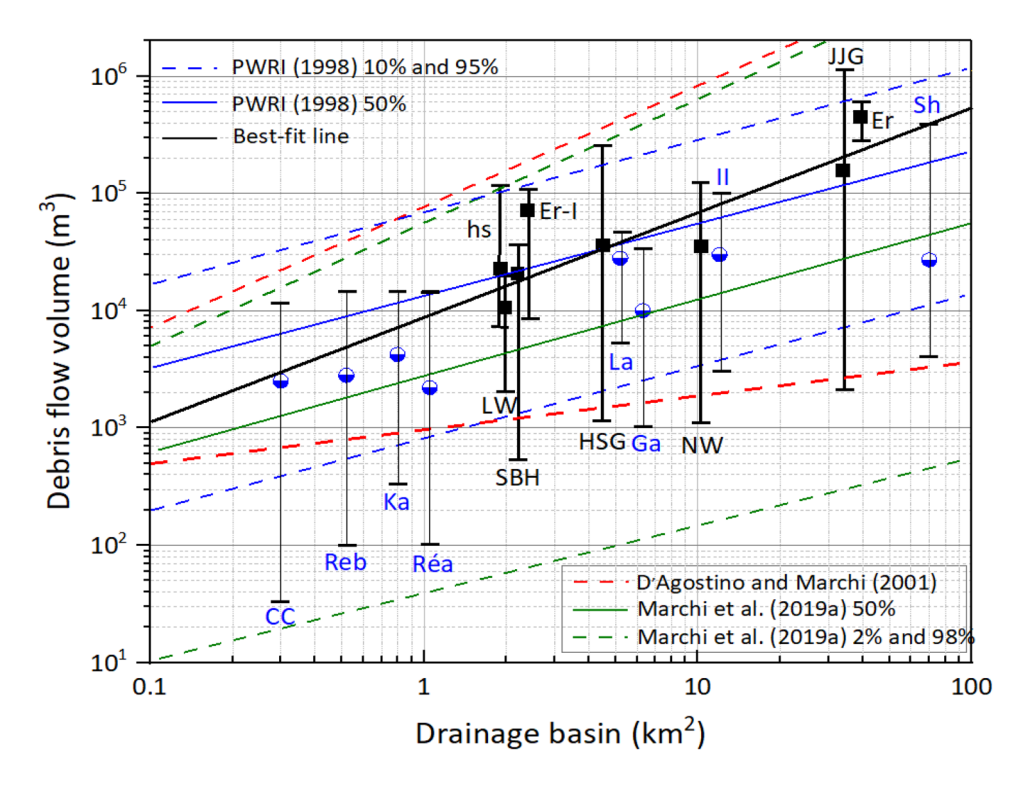


Fig. 8 Relationships between drainage basin area and debris flow volume. Average volumes are plotted, and error bars show the minimum and maximum values. See Fig. 3 and Table 2 for abbreviations of sites. Adapted from Hürlimann et al. (2019a, b)

## Peak discharge estimation

#### 1. Empirical methods for flow discharge calculation

Peak discharge is a crucial parameter for assessing the conveyance capacity of critical cross sections and for designing effective mitigation measures. To calculate the peak discharge of a debris flow, it is most useful to use known inducing parameters such as the empirical relationships established in previous literature between  $Q_p$  (peak discharge) and rainfall input, as well as debris flow volume (Hungr et al. 1984; Mizuyama et al. 1992; Takahashi et al. 1994). However, predicting debris flow discharge is highly challenging owing to the intricate physical processes involved and the inherent randomness of soil supply (Guo et al. 2020). The most reliable approach for determining the dynamics of a debris flow is through direct measurement of its actual movement in a natural setting. Initially, it entails assessing the cross-sectional area at the highest deposit level, together with the corresponding flow velocity. Consequently, a commonly employed equation can be formulated as follows:

$$Q_c = A_b V_c \tag{3}$$

where  $Q_{\rm c}$  is the flow discharge (m³/s), and  $A_{\rm b}$  and  $V_{\rm c}$  are the cross-sectional area (m²) and velocity at the cross section (m/s), respectively. This method can be applied only when specific monitoring data or evident field marks are available.

For channelized debris flows, peak discharge is related to water flow discharges:

$$Q_c = Q_B(1 + \psi) \tag{4}$$

where  $Q_B$  is the water flow discharge (m<sup>3</sup>/s), and  $\psi$  represents the solid concentration:

$$\psi = (\rho_c - 1)/(\rho_H - \rho_c) \tag{5}$$

where  $\rho_c$  and  $\rho_H$  are the density of the debris flow and solid materials, respectively.

The monitoring data support this relationship and help identify the parameters. For example, in the Ergou catchment, the ratio  $\psi$  ranges between 1.2 and 2.6.

To further account for the amplification effect, the equation can be modified as follows:

$$Q_{c} = Q_{B}(1 + \psi)\beta \tag{6}$$

Parameter  $\beta$  is known as the blockage ratio, which indicates the amplification effect of cross-sectional conditions (e.g., narrow sections and sharp curves) on discharge, and it traditionally falls within the range of 1.0–3.0. Generally, the parameter is identified empirically following field investigation.  $\beta$  = 1.0 means the case of debris floods and dilute debris flows. Conversely, higher values of  $\beta$  indicate viscous debris flows, with complex material supply and/or cross-sectional conditions that have the potential to amplify the flow discharge.

The aforementioned calculation, assuming that the discharge of a debris flow is a linear amplification of the water flow, is not applicable to the typical viscous debris flows in JJG. The ratio of debris flow discharge to water flow discharge in JJG exceeded 3.0 in many cases (with a maximum value reaching 15.6), according to field monitoring and hydrological modeling (Guo et al. 2020). This

ratio can aid in distinguishing between "normal" and "abnormal" debris flows. The hydrograph of the former type consists mainly of water with a small sediment volume, while that of the latter type exhibits markedly amplified peak discharge owing to blockage effects (Bardou 2002; Guo et al. 2020).

Equations (4) and (6) are also generally used for the calculation of peak discharge in the design of preventative works (Sichuan Hydrological Manual 1984; Zhou et al. 1991). However, estimating the peak discharge is highly challenging, even within a specific catchment, owing to uncertainties during the flow formation process. For example, it is acknowledged that antecedent rainfall, rainfall intensity, and landslide conditions all influence the peak discharge, and an empirical method is proposed as Eq. (7) for use in HSG (Zhang and Liu 1989):

$$Q_c = 1545(0.9i^{0.12} - 1) (7)$$

where i is the maximum 10-min rainfall intensity at P = 1% frequency. However, this calculation has no physical basis for application in other regions.

#### 2. Volume-peak discharge relationship

In many studies, the maximum debris flow volume has been considered in attempts to estimate the peak discharge for a given catchment (Hungr et al. 1984; Mizuyama et al. 1992; Takahashi et al. 1994; Rickenmann 1999; Jakob 2005). Generally, debris flow volume exhibits a power relation with peak discharge, and the relationships of the studied catchments in China and those of other catchments and/or regions worldwide are shown in Fig. 9 for comparison.

In JJG, each debris flow event consists of multiple surges. The volume-peak discharge relationships are markedly different when using the event and surge data. Using the volumes and peak discharges of the entire debris flow event (Line a) as the data source averages the surge process and lowers the relationship, compared with that derived using the volumes and peak discharges of each debris flow surge (Line b) as the data source. When using event data, which is a procedure that accords with most other related research, it is found that the best fit line of the event (Line a) closely resembles that in the Réa (Line 6) and Mos (Line 7) catchments, exhibiting a granular characteristic. Moreover, owing to the notably larger catchment area, it exhibits greater magnitude. The upper limit (Line a-1) is slightly higher than that for granular-type debris flows (Line 1, using the data from Switzerland, Ka, JJG, Mt. St. Helens, USGS flume, Lab experiments, and other field data, including lahars), whereas the lower limit (Line a-2) is slightly lower with the relationship observed at Sakurajima volcano (Line 5), showing a wide range.

The relationship of HSG (Line c) is grouped with the relationships representing mud flows (Line 3) and those representing volcanic debris flows that are primarily composed of fine material (Lines 4). These types of debris flow clearly have smaller peak discharges for a given volume in comparison to those of granulartype debris flows. This aligns with the characteristic of a mud flow regime in HSG.

Although the relationships in the small tributary Er-I (Line d-1) and the Ergou catchment (Line d-2) have different coefficients, the tendencies are similar, suggesting similarities in flow properties within the same catchment but at different scales. The relationships

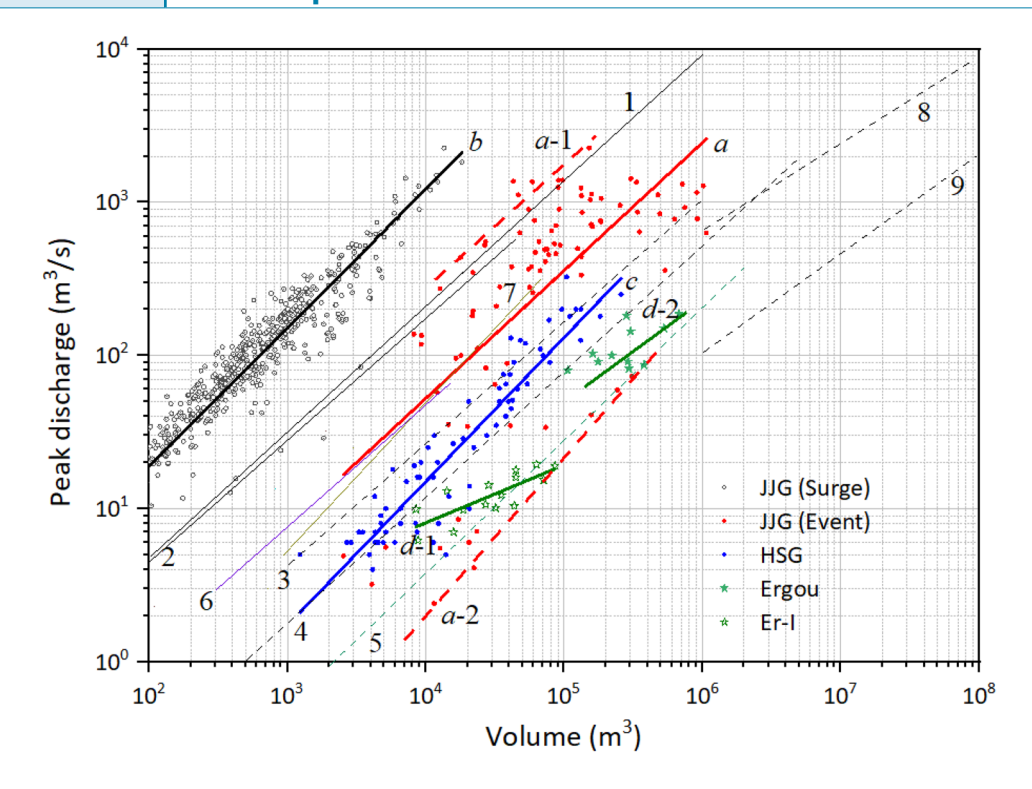


**Fig. 9** Empirical relationships between debris flow volume and peak discharge of the Chinese monitoring sites (Lines a, a-1, and a-2: the general relationship, and the upper and lower limits of the relationship in JJG, respectively, using the event peak discharge–volume as the data source; Line b: the relationship in JJG using the surge peak discharge–volume as the data source; Line c: the relationship in HSG; Lines d-1 and d-2: the relationship in the Ergou-1 and Ergou catchments, respectively). For comparison, data from sites outside China are also plotted (Lines 1–9 correspond to the data sources listed in Table 5). See Table 2 for abbreviations of sites

 Table 5
 Empirical formulas proposed for estimation of the relationship between debris flow peak discharge and volume

Data basis	Formula	Line in Fig. 10	N	R <sup>2</sup>	Source
JJG-1	$Q_{\rm p} = 0.0238 M_{\rm w}^{0.8355}$	(a)	555	0.44	
JJG-2	$Q_{\rm p} = 0.4905 M_{\rm w}^{0.8312}$	(b)	555	0.89	
HSG	$Q_{\rm p} = 0.0026^{0.9407}$	(c)	72	0.82	Zhang and Liu (1989)
ER-I	$Q_{\rm p} = 0.4623 M_{\rm w}^{0.4369}$	(d-1)	15	0.62	Cui et al. (2018)
ER	$Q_{\rm p} = 0.2495 M_{\rm w}^{0.3774}$	(d-2)	12	0.47	Cui et al. (2018)
Granular debris flows (worldwide dataset)	$Q_{\rm p} = 0.1 M^{0.833}$	(1)	145	nn	Rickenmann (1999)
Granular debris flows (Japan)	$Q_{\rm p} = 0.135 M^{0.780}$	(2)	~50	nn	Mizuyama et al. (1992)
Muddy debris flows (Japan)	$Q_{\rm p} = \text{o.o188} M^{\text{o.790}}$	(3)	~100	nn	Mizuyama et al. (1992)
Merapi volcano (Indonesia)	$Q_{\rm p} = 0.00558 M^{0.831}$	(4)	~200	0.95	Jitousono et al. (1996)
Sakurajima volcano (Japan)	$Q_{\rm p} = 0.00135 M^{0.870}$	(5)	~100	0.81	Jitousono et al. (1996)
Réal (France)	$Q_{\rm p} = 0.028 M_{\rm w}^{0.81}$	(6)	14	0.91	Navratil et al. (2013)
Moscado (Italy)	$Q_{\rm p} = 0.0055 M_{\rm w}^{0.9872}$	(7)	13	0.84	Marchi et al. (2002)
Landslide dam failures	$Q_{\rm p} = 0.293 M_{\rm w}^{0.56}$	(8)	9	0.73	Costa (1988)
Glacial dam failures	$Q_{\rm p} = 0.0163 M_{\rm w}^{0.64}$	(9)	20	0.80	Costa (1988)

exhibit smaller peak discharge for a given debris flow volume than in JJG and HSG, owing to the water-dominated debris flood/stony debris flow type.

It is worth mentioning that (1) the negative correlation between the BL catchments is difficult to establish owing to a lack of monitoring data, (2) the relationships of landslide dam failures (Line 8) and glacial dam failures (Line 9) are statistically significantly correlated with much greater total volume given a certain peak discharge, and all the catchments investigated in this work are not within this scope.

#### Rainfall conditions for debris flow triggering

Rainfall thresholds for debris flows have practical application in event forecasting. However, these thresholds exhibit marked variability, primarily because of regional variations of climate, morphology, vegetation cover, geology, and torrent control conditions. Additionally, predisposing factors related to the recent history of the catchment area (such as antecedent rainfall and sediment availability) contribute to this variability. Consequently, it is essential to consider that rainfall thresholds are typically site-specific. To better understand the controlling factors across the Chinese monitoring sites and the other global monitoring sites, we compared rainfall thresholds using the intensity–duration relationship and normalized the rainfall intensity by the MAP (Caine 1980; Guzzetti et al.

2007, 2008). Additionally, a positive relation between the hourly rainfall amount and the area of the drainage basin is observed, together with a possible scale effect (Guo et al. 2016c; Hürlimann et al. 2019a, b). For example, if the drainage basin is large but without abundant solid materials, some smaller debris flows might have deposited upstream, and only the largest events, triggered by the most intense rainfall, will be monitored, resulting in a higher rainfall threshold. Therefore, rainfall thresholds can reflect local debris flow susceptibility by considering MAP and local catchment scale.

As shown in Fig. 10, the results indicate that JJG exhibits relatively low values, although they are comparable to those of other sites such as La and Il. Notably, the monitoring areas of La and Il are 5.3 and 11.68 km<sup>2</sup>, respectively, whereas IIG covers a much larger area (33.4 km<sup>2</sup>). The Ergou catchment exhibits much higher thresholds than the other sites. On one hand, the larger watershed scale (39.4 km<sup>2</sup>) contributes to the phenomenon that smaller debris flows might have been deposited upstream of the monitoring station, meaning that only the largest events triggered by intense rainfall were detected. On the other hand, it is also attributable to stricter conditions regarding solid material mobilization in the channels. However, Ergou\*, representing the required rainfall conditions shortly after the occurrence of the Wenchuan earthquake, is similar to that of other sites, e.g., CC and Reb, with much smaller size. This reflects the impact of a large earthquake on debris flow activity, i.e., the threshold is substantially lower shortly after the earthquake and it gradually recovers with time (Guo et al. 2021b).

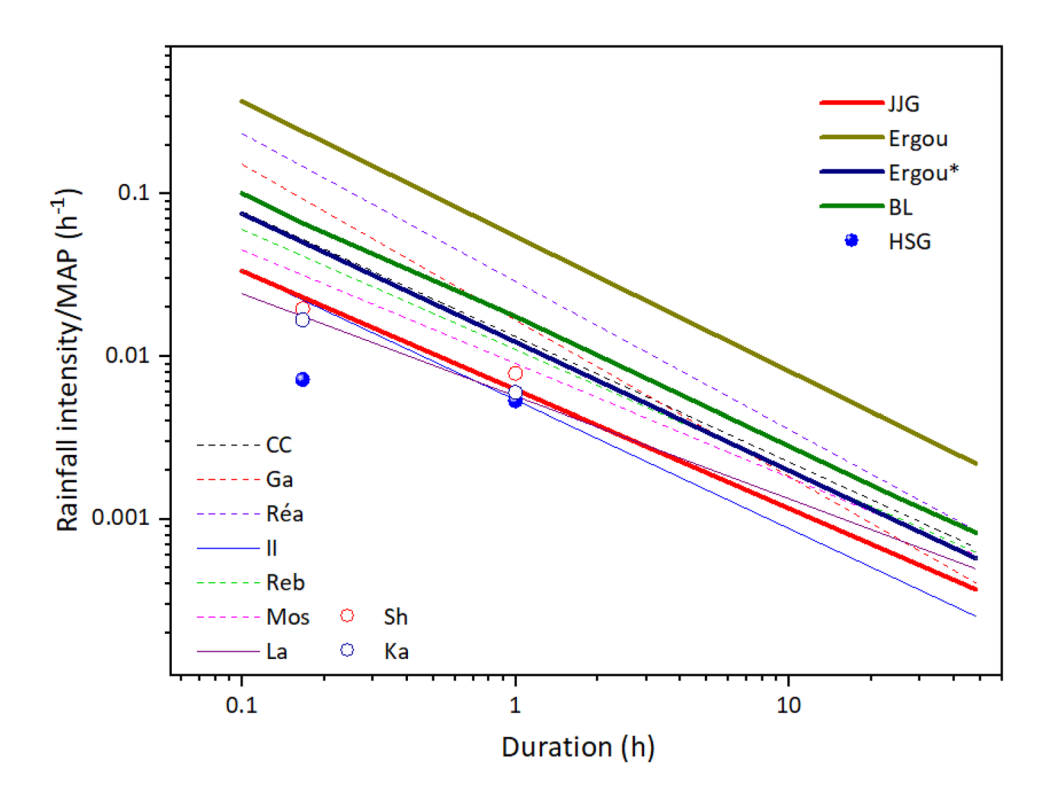


**Fig. 10** Comparison between mean normalized rainfall intensity by MAP and total duration threshold curves of the monitoring sites. See Table 2 for abbreviations of sites. Ergou\* represents the threshold defined under post-earthquake conditions in the Ergou catchment (Guo et al. 2016b). The rainfall thresholds of other sites refer to Coe et al. (2008, 2010), Guo et al. (2021b), Marchi et al. (2019b), McArdell and Badoux (2007), Badoux et al. (2009), Suwa et al. (2009), Navratil et al. (2013), Hübl et al. (2018), Bel et al. (2017), Hürlimann et al. (2019a, b), and Huang et al. (2013, 2017)

The rainfall intensity—duration relationship was not established in Illgraben (II), Lattenbach (La), and HSG, but critical rainfall amounts for durations of 10 min and 1 h were identified. Among these sites, HSG had the lowest critical rainfall amount owing to its close association with landsliding activities and the notable influence of antecedent soil water content conditions on catchment behavior. It is proposed that the rainfall required for triggering soil movement is as low as 1.8 mm/10 min, which aligns closely with the stable infiltration rate of the soil.

We wish to stress that some of the variability in the intensity-duration threshold is likely attributable to the data sources and the methodologies used to define the threshold, as has been discussed in many previous studies (e.g., Nikolopoulos et al. 2015; Segoni et al. 2018). Moreover, rainfall thresholds strongly depend on the initiation process. In most sites, debris flows are triggered primarily by surface runoff; however, those in JJG and HSG are typically landslide-driven (Guo et al. 2021a, b). Because the relationship between rainfall and the triggering of debris flows is highly complex and nonlinear, other factors must be considered, e.g., in particular, local hydrological conditions, slope morphology, and vegetation cover. It is not possible to define a unique threshold, even for supply-unlimited systems (Guo et al. 2020; Hürlimann et al. 2019a, b); however, thresholds can reflect local debris flow susceptibility and provide a reference for developing an early warning system.

#### **Final remarks**

Debris flow monitoring is a crucial task for enhancing our comprehension of initiation mechanisms, flow dynamics, and hazard risk. This study provided an overview of the monitoring outputs in seven catchments in China. The monitoring catchments are generally larger than those of other sites worldwide, with different flow regimes in different regions. Monitoring data, mostly obtained using the manual approach, have provided valuable datasets for the historical period. These data helped build the relationships for the calculation of flow velocity, discharge, and total volume. The following points emerged as key concerns from this review and analysis of the monitoring data.

- 1. The definitions used for debris flows in China are consistent with Western descriptions in terms of formation conditions, material composition, and movement patterns, but classifications based on rheological parameters differ. Moreover, the specific meanings of hyperconcentrated flows are different. Additionally, the term debris flood is not used in China, and debris flows are commonly sub-divided into dilute debris flows, subviscous debris flows, and viscous debris flows by taking the density and clay-water ratio as the two primary defining parameters.
- 2. In the Jiangjia Gully and Bailong River regions, the formation of debris flows is predominantly landslide-driven from various failures. In the Hunshui Gully, debris flows primarily originate from erosion on specific highly weathered ancient landslides with a substantial proportion of clays and fine particles. In the Ergou catchment, debris flows are primarily runoff-driven. The differences in the formation processes determine the various debris flow regimes and dynamic characteristics.
- The GSDs exhibit notably broader spectra, and the flows behave as viscoplastic flows with density of up to 2.4 g/cm³ in Jiangjia Gully and the Bailong River catchments. The volume-peak dis-

charge relationship shows a wide range, and the best fit line exhibits a granular-type debris flow characteristic. In Hunshui Gully, the flow regime represents a mud flow with particles concentrated within a specific range and composed of abundant clay in most cases. Moreover, the volume-peak discharge relationship is grouped with those representing mud flows. In the Ergou catchment, the particle compositions include less clay and more coarse sands and gravels, which are better suited to a collisional-frictional regime. The flows behave more like stony debris flows or debris floods, exhibiting smaller peak discharge for a given debris flow volume than in Jiangjia Gully and Hunshui Gully.

- 4. The velocity-depth relationship in Jiangjia Gully varies between events, but with a much higher upper limit than that observed for other sites owing to the resistance reduction of viscous debris flows, in which the process of paving the way contributes substantially. Both the velocity-depth relationship and the F<sub>r</sub> value are higher in viscoplastic debris flows (i.e., in the Jiangjia Gully and Bailong River catchments), intermediate in mud flows (Hunshui Gully), and lower in debris floods (the Ergou catchment).
- 5. Comparison of the rainfall thresholds following normalization with the mean annual precipitation showed that the Ergou catchment has much higher rainfall thresholds than the other sites and that Jiangjia Gully and the tributaries of the Bailong River have lower threshold values, indicating their different susceptibility to debris flow occurrence.
  - The GSD of debris flows in Gadria-1, Chalk Cliffs, and Shenmu generally falls in or is close to the range of that in Ergou and Shenmu, indicating a collisional-frictional regime, and those in other international monitoring sites fall in the range of that in Bailong and Hunshuigou, indicating similar regimes characterized by viscoplastic flows. The flow velocity-depth relation and  $F_r$  values in the Chinese sites are generally higher than those for international sites. This result might include uncertainties attributable to differences in flow regimes, channel conditions, and data sources. The volume-basin area relationships are all higher than the 50th percentile line but remain within the envelopes proposed for worldwide sites (D'Agostino and Marchi 2001; Marchi et al. 2019a), whereas the maximum and the average debris flow volumes of Chinese sites are generally higher than those of other sites with similar catchment size. In comparison, the rainfall threshold of Ergou is higher than that of all other sites, whereas Jiangjia Gully has a very low threshold that is close to that of the La and Il sites, despite its much larger drainage area.

Notably, the monitoring sites are successful with effective data up to date, and the outputs help understand the rainfall-induced debris flow behaviors. Increasing numbers of new monitoring sites, including sites monitoring glacial debris flows on the Tibetan Plateau, have also drawn increasing concern in recent years; however, analyses of the data of such sites are not mentioned owing to the relatively limited monitoring results to date. Another consideration is that research on debris flows often requires long-term monitoring data, and except for a few sites (e.g., Jiangjia and Kamikamihorizawa) that had monitoring instruments installed in the 1960s and 1970s, most monitoring systems in watersheds worldwide were

established at around the turn of the twenty-first century. In this sense, the manual monitoring is of particular importance. The historical monitoring data facilitate comprehension of the dynamics and regional variations in debris flow characteristics and risks. Furthermore, they support the prediction of future risks arising from climate change and human activities, especially in densely populated mountainous areas in western China.

#### **Acknowledgements**

We thank James Buxton MSc, from Liwen Bianji (Edanz) (www.liwenbianji.cn/), for editing the English text of a draft of this manuscript.

## **Funding**

This study was supported by the Second Scientific Expedition on the Qinghai–Tibet Plateau (2019QZKK0903-02), NSFC (42322703 and 41925030), the Western Light of Young Scholars, CAS, and Sichuan Outstanding young talent project (2022JDJQ0008).

#### **Data availability**

The data that support the findings of this study are available from the authors, upon reasonable request.

#### Declarations

**Conflict of interest** The authors declare no competing interests.

#### References

- Abancó C, Hürlimann M, Fritschi B, Graf C, Moya J (2012) Transformation of ground vibration signal for debris-flow monitoring and detection in alarm systems. Sensors 12:4870–4891
- Abancó C, Hürlimann M, Moya J (2014) Analysis of the ground vibration generated by debris flows and other torrential processes at the Rebaixader monitoring site (Central Pyrenees, Spain). Nat Hazards Earth Syst Sci Discuss 14:929–943
- Abancó C, Hürlimann M, Moya J, Berenguer M (2016) Critical rainfall conditions for the initiation of torrential flows. Results from the Rebaixader catchment (Central Pyrenees). J Hydrol (amst) 541:218–229
- Allstadt KE, Farin M, Iverson RM, Obryk MK, Kean JW, Tsai VC et al (2020) Measuring basal force fluctuations of debris flows using seismic recordings and empirical Green's functions. J Geophys Res Earth Surf 125:e2020JF005590
- Arattano M, Moia F (1999) Monitoring the propagation of a debris flow along a torrent. Hydrol Sci J 44:811–823
- Arattano M, Coviello V, Cavalli M, Comiti F, Macconi P, Theule J, Crema S (2015) Brief communication: a new testing field for debris flow warning systems. Nat Hazards Earth Syst Sci Discuss 15:1545–1549
- Badoux A, Graf C, Rhyner J, Kuntner R, McArdell B (2009) A debrisflow alarm system for the Alpine Illgraben catchment: design and performance. Nat Hazards 517–539
- Bardou E, Ancey C, Bonnard C, Vulliet L (2003) Classification of debris-flow deposits for hazard assessment in alpine areas. In: Rickenmann D, Chen C-L (eds) Debris flow hazards mitigation: mechanics prediction and assessment. Millpress, Rotterdam, Davos (Switzerland), pp 799–808
- Bardou E (2002) Methodologie de Diagnostic des laves torrentielles surun bassin versant alpin. EPFL, Lausanne
- Bel C, Liébault F, Navratil O, Eckert N, Bellot H, Fontaine F, Laigle D (2017) Rainfall control of debris-flow triggering in the Réal Torrent, Southern French Prealps. Geomorphology 291:17–32

- Belli G, Walter F, McArdell B, Gheri D, Marchetti E (2022) Infrasonic and seismic analysis of debris-flow events at Illgraben (Switzerland): relating signal features to flow parameters and to the seismo-acoustic source mechanism. J Geophys Res Earth Surf 127:e2021JF006576
- Berti M, Genevois R, Simoni A, Tecca PR (1999) Field observations of a debris flow event in the Dolomites. Geomorphology 29:265–274
- Berti M, Genevois R, La Husen R, Simoni A, Tecca PR (2000) Debris flow monitoring in the Acquabona watershed on the Dolomites (Italian Alps). Phys Chem Earth 25:707–715
- Bertrand M, Liébault F, Piégay H (2013) Debris-flow susceptibility of upland catchments. Nat Hazards 67:497–511
- Beverage JP, Culbertson JK (1964) Hyperconcentrations of suspended sediment. Hydraul Div Am Soc Civ Eng HY6:117-126
- Bremer M, Sass O et al (2012) Combining airborne and terrestrial laser scanning for quantifying erosion and deposition by a debris flow event. Geomorphology 138:49–60
- Brenna A, Surian N, Ghinassi M, Marchi L (2020) Sediment-water flows in mountain streams: recognition and classification based on field evidence. Geomorphology 371:107413
- Caine N (1980) The rainfall intensity-duration control of shallow landslides and debris flows. Geogr Ann Ser B 62:23–27
- Catani F, Canuti P, Casagli N (2014) The use of radar interferometry in landslide monitoring. In: Shan W, Guo Y, Wang F, Marui H, Strom A (Eds.), Landslides in cold regions in the context of climate change. Springer, pp. 177–190
- Chen GX, Wang JK, Wang LH (1983) Debris flow prevention. China Railway Publishing House, Beijing (in Chinese)
- Chen Q, Song D, Chen X, Zhong W (2023) Visco-collisional scaling law of flow resistance and its application in debris-flow mobility. J Geophys Res Earth Surf 128:e2022JF006712
- Church M, Jakob M (2020) What is a debris flood? Water Resources Research
- Coe JA, Kinner DA, Godt JW (2008) Initiation conditions for debris flows generated by runoff at Chalk Cliffs, central Colorado. Geomorphology 96:270–297
- Coe JA, Kean JW, McCoy SW, Staley DM, Wasklewicz TA (2010) Chalk Creek Valley: Colorado`s natural debris-flow laboratory. In: Morgan, L., Quane, S. (Eds.), Through the Generations: Geologic and Anthropogenic Field Excursions in the Rocky Mountains from Modern to Ancient Geological Society of America Field Guide 18, pp. 95–117
- Comiti F, Marchi L, Macconi P, Arattano M, Bertoldi G, Borga M, Brardinoni F, Cavalli M, D'Agostino V, Penna D, Theule J (2014) A new monitoring station for debris flows in the European Alps: first observations in the Gadria basin. Nat Hazards 73:1175–1198
- Cook KL (2017) An evaluation of the effectiveness of low-cost UAVs and structure from motion for geomorphic change detection.

  Geomorphology 278:195–208
- Costa JE (1984) Physical geomorphology of debris flows. In: Costa JE, Fleischer PJ (eds) Developments and Applications of Geomorphology. Springer, Berlin, Germany, pp 268–317
- Costa JE (1988) Floods from dam failures, In: V. R. Baker et al. (eds), Flood Geomorphology, John Wiley & Sons, New York, pp. 439–463
- Coussot P, Meunier M (1996) Recognition, classification and mechanical description of debris flows. Earth-Sci Rev 40(209):182–227
- Coviello V, Arattano M, Marchi L, Comiti F, Macconi P (2019a) Seismic characterization of debris flows: insights into energy radiation and implications for warning. J Geophys Res Earth Surf 124(6):1440–1463
- Coviello V, Theule JI, Marchi L, Comiti F, Crema S, Cavalli M, Arattano M, Lucía A, Macconi P (2019b) Deciphering sediment dynamics in a debris-flow catchment: insights from instrumental monitoring and high-resolution topography. In: 7th International Conference on Debris-Flow Hazards Mitigation. Boulder, CO

- Cucchiaro S, Cavalli M, Vericat D, Crema S, Llena M, Beinat A, Marchi L, Cazorzi F (2018) Monitoring topographic changes through 4D-structure-from-motion photogrammetry: application to a debris-flow channel. Environ Earth Sci 77:632
- Cui P, Chen XQ, Zhu YY, Su FH, Wei FQ, Han YS, Liu HJ, Zhuang JQ (2011) The Wenchuan earthquake (May 12, 2008), Sichuan Province, China, and resulting geohazards. Nat Hazards 56(1):19–36
- Cui P, Zhou GG, Zhu XH, Zhang JQ (2013) Scale amplification of natural debris flows caused by cascading landslide dam failures. Geomorphology 182:173–189
- Cui P, Zhang JQ, Yang ZJ, Chen XQ, You Y, Li Y (2014) Activity and distribution of geohazards induced by the Lushan earthquake, April 20, 2013. Nat Hazards 73:711–726
- Cui P, Guo X, Yan Y, Li Y, Ge Y (2018) Real-time observation of an active debris flow watershed in the Wenchuan earthquake area. Geomorphology 321:153–166
- D'Agostino V, Marchi L (2001) Debris flow magnitude in the Eastern Italian Alps: data collection and analysis. Phys. Chem. Earth, Part C Solar. Terr Planet Sci 26:657–663
- De Haas T, Ventra D, Carbonneau PE, Kleinhans MG (2014) Debrisflow dominance of alluvial fans masked by runoff reworking and weathering. Geomorphology 217:165–181
- Gregoretti C, Degetto M, Bernard M, Crucil G, Pimazzoni A, De Vido G, Berti M, Simoni A, Lanzoni S (2016) Runoff of small rocky headwater catchments: field observations and hydrological modeling. Water Resour Res 52:8138–8158
- Gregoretti C, Stancanelli LM, Bernard M, Boreggio M, Degetto M, Lanzoni S (2019) Relevance of erosion processes when modelling in-channel gravel debris flows for efficient hazard assessment. J Hydrol 575–591
- Guo XJ, Cui P, Li Y, Ma L, Ge YG, William BM (2016a) Intensity-duration threshold of rainfall triggering debris flows in Wenchuan earthquake area, China. Geomorphology 263:208–216
- Guo XJ, Cui P, Li Y, Zou Q, Kong YD (2016b) The formation and development of debris flows in large watersheds after the 2008 Wenchuan earthquake. Landslides 13:25–37
- Guo XJ, Cui P, Li Y, Zhang JQ, Ma L, William BM (2016c) Spatial features of debris flows and their rainfall thresholds in the Wenchuan earthquake-affected area. Landslides 13:1215–1229
- Guo XJ, Li Y, Cui P, Yan H, Zhuang JQ (2020) Intermittent viscous debris flow formation in Jiangjia Gully from the perspectives of hydrological processes and material supply. J Hydrol 589:125184
- Guo XJ, Chen XC, Song GH, Zhuang JQ, Fan JL (2021a) Debris flows in the Lushan earthquake area: formation characteristics, rainfall conditions, and evolutionary tendency. Nat Hazards 106(3):2663–2687
- Guo XJ, Li Y, Chen XC, Zhang J, Sun YQ (2021b) Variation of debris flow/ flood formation conditions at the watershed scale in the Wenchuan earthquake area. Landslides 18:2427–2443
- Guzzetti F, Peruccacci S, Rossi M, Stark C (2007) Rainfall thresholds for the initiation of landslides in central and southern Europe. Meteorol Atmos Phys 98:239–2125
- Guzzetti F, Peruccacci S, Rossi M, Stark C (2008) The rainfall intensity–duration control of shallow landslides and debris flows: an update. Landslides 5:3–17
- Hu KH, Wei FQ, Li Y, Cui P (2004) Characteristics of debris-flow surge. J Mt Sci 22(6):707-712
- Huang YM, Chen WC, Fang YM, Lee BJ, Chou TY, Yin H (2013) Debris flow monitoring a case study of Shenmu Area in Taiwan. Disasters Adv 6:1–9
- Huang T, Ding MT, Gao ZM, Téllez RD (2021) Check dam storage capacity calculation based on high-resolution topogrammetry: case study of the Cutou Gully, Wenchuan County. China Science of the Total Environment 790
- Huang YM, Fang Y, Chou T, Lee C, Yin H (2017) The vibration signal analysis of debris flow in Taiwan. In: 5th International Conference

- on Geotechnical Engineering for Disaster Mitigation and Rehabilitation. Taipei, Taiwan. pp. 13–14
- Hübl J, Kaitna R (2010) Sediment delivery from the Lattenbach catchment by debris floods and debris flows. EGU General Assembly. p. 10585
- Hübl J, Mikoš M (2018) Practice guidelines on monitoring and warning technology for debris flows. In: Sassa, K., Guzzetti, F., Yamagishi, H., Arbanas, Ž., Casagli, N., McSaveney, M., Dang, K. (Eds.), Landslide Dynamics: ISDR-ICL Landslide Interactive Teaching Tools. Springer Nature, pp. 567–585
- Hübl J, Suda J, Proske D, Kaitna R, Scheidl C (2009) Debris flow impact estimation. In: Popovska C, Jovanovski M (Eds.), 11th Symposium on Water Management and Hydraulic Engineering. Ohrid, Macedonia. pp. 137–148
- Hübl J, Schimmel A, Koschuch R (2018) Evaluation of different methods for debris flow velocity measurements at the Lattenbach Creek. INTERPRAEVENT 2018. pp. 2–8 Toyama, Japan, Japan
- Hungr O, Evans SG, Bovis MJ, Hutchinson JN (2001) A review of the classification of landslides of the flow type. Environ Eng Geosci 7:221–238
- Hungr O, Jakob M (2005) Debris flows hazards and related phenomena. Springer, Praxis, p 728
- Hungr O, Morgan GC, Kellerhals R (1984) Quantitative analysis of debris torrent hazards for design of remedial measures. Can Geotechnical J 21:663-677
- Hungr O, Leroueil S, Picarelli L (2014) The Varnes classification of landslide types, an update. Landslides 11(2):167–194
- Hürlimann M, Rickenmann D, Graf C (2003) Field and monitoring data of debris-flow events in the Swiss Alps. Can Geotech J 40:161–175
- Hürlimann M, Abancó C, Moya J, Vilajosana I (2014) Results and experiences gathered at the Rebaixader debris-flow monitoring site, Central Pyrenees, Spain. Landslides 11:939–953
- Hürlimann M, Coviello V, Bel C, Guo X, Berti M, Graf C, Hübl J, Miyata S, Smith JB, Yin HY (2019a) Debris-flow monitoring and warning: review and examples. Earth Sci Rev 199:102981
- Hurlimann Ziegler M, Oorthuis Gómez R, Abanco Martínez de Arenzana C, Carleo L, Moya Sánchez J et al (2019) Monitoring of rainfall and infiltration at the Rebaixader catchment (Central Pyrenees). In: Kean W.J. (Ed.), 7th International Conference on Debris-Flow Hazards Mitigation. AEG, pp. 131–137
- Imaizumi F, Tsuchiya S, Ohsaka O (2005) Behaviour of debris flows located in a mountainous torrent on the Ohya landslide. Japan Can Geotech J 42:919–931
- Itakura Y, Inaba H, Sawada T (2005) A debris-flow monitoring devices and methods bibliography. Nat Hazards Earth Syst Sci 5:971–977
- Jacquemart M, Meier L, Graf C, Morsdorf F (2017) 3D dynamics of debris flows quantified at sub-second intervals from laser profiles. Nat Hazards 89:785–800
- Jakob M (2005) A size classification for debris flows. Eng Geol 79:151–161Jakob M, Hungr O (2005) Debris-flow hazards and related phenomena.Springer, Berlin, p 739
- Jitousono T, Shimokawa E, Tsuchiya S (1996) Debris flow following the 1994 eruption with pyroclastic flows in Merapi volcano, Indonesia, J Jap Soc Erosion Control Engng 48(Special Issue), 109–116
- Johnson AM (1970) Physical processes in geology. Freeman and Cooper, San Francisco 577
- Kang ZC, Li ZF, Ma AN, Hu JT (2004) Research on debris flow in China. Science Publishing House (in Chinese), Beijing
- Kang ZC (1985) Velocity analysis of viscous debris flow in Jiangjiagou, Dongchuan, Yunnan Province. Journal of Lanzhou Institute of Glaciology and Geocryology, Chinese Academy of Sciences (4). Science Press. Beijing, 108–117 (in Chinese)
- Kean JW, Staley DM, Cannon SH (2011) In situ measurements of postfire debris flows in southern California: comparisons of the timing and magnitude of 24 debrisflow events with rainfall and soil moisture conditions. J Geophys Res 116(F4):F04019

- Kean JW, McCoy SW, Tucker GE, Staley DM, Coe JA (2013) Runoffgenerated debris flows: observations and modeling of surge initiation, magnitude, and frequency. J Geophys Res Earth Surf 118
- Li Y, Yao SF, Hu KH, Chen XQ, Cui P (2003) Surges and deposits of debris flow in Jiangjia Gully. J Mountain Sci 21(6):712-715
- Li HL, Zeng SQ (1982) Debris flow in Gansu Province. Publishing House of People`s Transportation. Beijing
- Li Y, Hu KH, Yue ZQ, Tham TG (2004) Termination and deposition of debris-flow surge. Landslides: evaluation and stabilization. Taylor & Francis Group, London, 1451–1456
- Manville V, Hodgson KA, White JDL (1998) Rheological properties of a remobilized tephra lahar associated with the 1995 eruptions of Ruapehu volcano, New Zealand. New Zealand J Geol Geophys 41:157–164
- Manville V, White JDL (2003) Incipient granular mass flows at the base of sedimentladen floods, and the roles of flow competence and flow capacity in the deposition of stratified bouldery sands. Sediment. Geol 155(1–2):157–173
- Marchetti E, Walter F, Barfucci G, Genco R, Wenner M, Ripepe M et al (2019) Infrasound array analysis of debris flow activity and implication for early warning. J Geophys Res Earth Surf 124:567–587
- Marchi L, Arattano M, Deganutti AM (2002) Ten years of debris-flow monitoring in the Moscardo Torrent (Italian Alps). Geomorphology 46:1–17
- Marchi L, Brunetti MT, Cavalli M, Crema S (2019a) Debris-flow volumes in northeastern Italy: relationship with drainage area and size probability. Earth Surf Process Landforms 44(4):933-943
- Marchi L, Coviello V, Comiti F, Crema S, Cavalli M, Macconi P (2019b) Rainfall threshold for debris flow occurrence in the Gadria catchment, eastern Italian Alps. Geophys Res Abstr EGU 2019–7188
- McArdell B, Badoux A (2007) Influence of rainfall on the initiation of debris flows at the Illgraben catchment, canton of Valais, Switzerland. Geophys Res Abstr 9: 8804
- McArdell BW (2016) Field measurements of forces in debris flows at the Illgraben: implications for channel-bed Erosion. Int J Eros Control Eng 9:194–198
- McCoy SW, Kean JW, Coe JA, Staley DM, Wasklewicz TA, Tucker GE (2010) Evolution of a natural debris flow: in situ measurements of flow dynamics, video imagery, and terrestrial laser scanning. Geology 38:735-738
- McCoy SW, Coe JA, Kean JW, Tucker GE, Staley DM, Wasklewicz TA (2011) Observations of debris flows at Chalk Cliffs, Colorado, USA: part 1, in situ measurements of flow dynamics, tracer particle movement and video imagery from the summer of 2009. Ital J Eng Geol Environ 65–75
- McCoy SW, Kean JW, Coe JA, Tucker GE, Staley DM, Wasklewicz TA (2012) Sediment entrainment by debris flows: in situ measurements from the headwaters of a steep catchment. J Geophys Res 117:F03016
- McCoy SW, Tucker GE, Kean JW, Coe JA (2013) Field measurement of basal forces generated by erosive debris flows. J Geophys Res Earth Surf 118:589–602
- Mizuyama T, Kobashi S, Ou G (1992) Prediction of debris flow peak discharge, Proc Int Symp Interpraevent, Bern, Switzerland 4:99–108
- Morino C, Conway SJ, Balme MR, Hillier J, Jordan C, Sæmundsson Þ, Argles T (2019) Debris-flow release processes investigated through the analysis of multi-temporal LiDAR datasets in northwestern Iceland. Earth Surf Process Landforms 44:144–159
- Nagl G, Kaitna R, Hübl J (2018) A monitoring barrier for investigating debris flow/ structure/ground interactions. 5th Int Conf Debris Flows Disasters, Risk, Forecast Prot 152–157
- Nagl G, Hübl J (2017) A check-dam to measure debris flow-structure interactions in the Gadria torrent. In: Mikoš M, Vilímek V, Yin Y, Sassa K (eds) Advancing culture of living with landslides. Springer International Publishing, Cham, pp 465–471

- Navratil O, Liébault F, Bellot H, Travaglini E, Theule J, Chambon G, Laigle D (2013) High-frequency monitoring of debris-flow propagation along the Réal Torrent, Southern French Prealps. Geomorphology 201:157–171
- Nikolopoulos EI, Borga M, Creutin JD, Marra F (2015) Estimation of debris flow triggering rainfall: Influence of rain gauge density and interpolation methods. Geomorphology 243:40-50
- Okano K, Suwa H, Kannno T (2012) Characterization of debris flows by rainstorm condition at a torrent on the Mount Yakedake volcano, Japan. Geomorphology 136:88–94
- Palau RM, Hürlimann M, Pinyol J, Moya J, Victoriano A, Génova M, Puig C (2017) Recent debris-flows in the Portainé catchment (Eastern Pyrenees, Spain). Analysis of monitoring and field data focussing on the 2015 event. Landslides 14:1161–1170
- Pierson TC (1980) Debris flows: an important process in high country gully erosion. J Tussok Grassland MT Lands Inst (N.Z.) 39:3-14
- Pierson TC, Costa JE (1987) A rheologic classification of subaerial sediment-water flows. In: Costa JE, Wieczorek GF (Eds), Debris Flows/Avalanches: Process, Recognition, and Mitigation. Reviews in Engineering Geology. Vol. 7. The Geological Society of America, Boulder, CO: 1–12
- PWRI (1988) Technical standard for measures against debris flow (draft), Technical Memorandum of PWRI, No. 2632, Ministry of Construction, Japan
- Qian N, Wang ZY (1984) A preliminary study on the mechanism of debris flows. Acta Geogr Sin 39(1):33-43 (in Chinese)
- Waananen AO, Harris DD, Williams RC (1970) Floods of December 1964 and January 1965 in the Far Western States: Part 2. Streamflow and Sediment Data (861 pp). Department of the Interior, US Geological Survey, Reston, VA: US
- Rickenmann D (1999) Empirical relationships for debris flows. Nat Hazards 19:47–77
- Rickenmann D (1991) Hyperconcentrated flow and sediment transport at steep slopes. J Hydr Engng ASCE 117(11):1419–1439
- Scheidl C, Rickenmann D (2010) Empirical prediction of debris-flow mobility and deposition on fans. Earth Surf Process Landf 35(2):157-173
- Segoni S, Piciullo L, Gariano SL (2018) A review of the recent literature on rainfall thresholds for landslide occurrence. Landslides 15(8):1483–1501
- Sichuan Hydrological Manual (1984) Rainstorm-runoff calculation method in small watershed, 1984, Sichuan Water Conservancy and Power Department. Electronic publishing. (in Chinese)
- Suwa H, Okano K, Kanno T (2009) Behavior of debris flows monitored on test slopes of Kamikamihorizawa Creek, Mount Yakedake. Japan Int J Eros Control Eng 2:33-45
- Suwa H, Okano K, Kanno T (2011) Forty years of debris-flow monitoring at Kamikamihorizawa Creek, Mount Yakedake. In: Genevois, R., Hamilton, D.L., Prestininzi, A. (Eds.), 5th International Conference on Debris-Flow Hazards Mitigation. Padua. pp. 605–613
- Takahashi T (1991) Debris flow, Monograph of IAHR, AA Balkema Rotterdam
- Takahashi T, Sawada T, Suwa H, Mizuyama T, Mizuhara K, Wu J, Tang B, Kang Z, Zhou B (1994) Japan-China joint research on the prevention from debris flow hazards, Research Report, Japanese Ministry of Education, Science and Culture, Int. Scientific Research Program No. 03044085
- Tang B, Zhou BF, Wu JS (2000) Debris flow in China. The Commercial Press (in Chinese), Beijing
- Tang C, van Asch TWJ, Chang M, Chen GQ, Zhao XH, Huang XC (2012) Catastrophic debris flows on 13 August 2010 in the Qingping area, southwestern China: the combined effects of a strong earthquake and subsequent rainstorms. Geomorphology 139–140:559–576
- Thouret JC, Antoine S, Magill C, Ollier C (2020) Lahars and debris flows: characteristics and impacts. Earth-Sci Rev 201:103003

- Vallance JW et al (2000) Lahars. In: Sigurdsson H (ed) Encyclopedia of Volcanoes, first edit. Academic Press, San Diego, pp 601–615
- Vallance JW, Iverson R et al (2015) Lahars and their deposits. In: Sigurdsson H (ed) Encyclopedia of Volcanoes, 2nd edit. Academic Press, San Diego, pp 649–664
- Wang ZY, Cui P, Yu B (2001) The mechanism of debris flow and drag reduction. Journal of Natural Disasters 10(3):37-43 (in Chinese)
- Wei SC, Liu KF (2020) Automatic debris flow detection using geophones. Landslides 17:349-359
- Wendeler C, Volkwein A, Roth A, Denk M, Wartmann S (2007) Field measurements and numerical modelling of flexible debris flow barriers. Debris-flow hazards mitigation: mechanics prediction and assessment. pp. 681–687
- Wilford DJ, Sakals ME, Innes JL, Sidle RC, Bergerud WA (2004) Recognition of debris flow, debris flood and flood hazard through watershed morphometrics. Landslides 1:61–66
- Wu JS, Tian LQ, Kang ZC, Zhang YF, Liu J (1993) Debris flow and its comprehensive measurement. Science Press, Beijing (in Chinese)
- Yan Y, Tang H, Hu K, Turowski JM, Wei F (2023) Deriving debris-flow dynamics from real-time impact-force measurements. J Geophys Res Earth Surf 128:e2022JF006715
- Yang F, Fan X, Siva Subramanian S, Dou X, Xiong J, Xia B, Xu Q (2021) Catastrophic debris flows triggered by the 20 August 2019 rainfall, a decade since the Wenchuan earthquake. China Landslides 18(9):3197–3212
- Yang ZN (1985) A preliminary study on the velocity formula of rainfall-induced viscous debris flow. Journal of Lanzhou Institute of Glaciology and Geocryology, Chinese Academy of Sciences (4). Science Press. Beijing, 199–206 (in Chinese)
- Yin HY, Huang CJ, Chen CY, Fang YM, Lee BJ, Chou TY (2011) The present development of debris flow monitoring technology in Taiwan a case study presentation. In: Genevois, R., Hamilton,

- D., Prestininzi, A. (Eds.), 5th Int. Conf. on Debris-Flow Hazards Mitigation. Padua. pp. 623–631
- Yu GA, Yao W, Huang HQ, Liu Z (2020) Debris flows originating in the mountain cryosphere under a changing climate: a review. Progress in Physical Geography: Earth and Environment, 030913332096170
- Zanchetta G, Sulpizio R, Pareschi MT, Leoni FM, Santacroce R (2004) Characteristics of May 5–6,1998 volcaniclastic debris flows in the Sarno area (Campania, southern Italy): relationships to structural damage and hazard zonation. J Volc Geoth Res 133:377–393
- Zhang XB, Liu J (1989) Debris flow in Hunshui Gully, Yingjiang River. Chengdu Map Press, Chengdu, Yunnan Province
- Zhou BF, Li DJ, Luo DF (1991) Guide to prevention of debris flow. Science Press, Beijing (In Chinese)

Springer Nature or its licensor (e.g. a society or other partner) holds exclusive rights to this article under a publishing agreement with the author(s) or other rightsholder(s); author self-archiving of the accepted manuscript version of this article is solely governed by the terms of such publishing agreement and applicable law.

### Xiaojun Guo (☑) · Peng Cui · Xiaoqing Chen · Yong Li

Key Laboratory of Mountain Hazards and Surface Process/Institute of Mountain Hazards and Environment, Chinese Academy of Sciences, Chengdu 610041, China Email: aaronguo@imde.ac.cn

#### Marcel Hürlimann

Department of Civil and Environmental Engineering, UPC Barcelona TECH, Barcelona, Spain